Deep Sea Research Part II: Topical Studies in Oceanography
August 2017, Volume 142, Pages 7-24
http://dx.doi.org/10.1016/j.dsr2.2016.05.006
http://archimer.ifremer.fr/doc/00335/44580/

The Congolobe project, a multidisciplinary study of Congo deep-sea fan lobe complex: Overview of methods, strategies, observations and sampling

Rabouille C. [1, *], Olu Karine [2], Baudin F. [3], Khripounoff Alexis [2], Dennielou Bernard [4], Arnaud-Haond Sophie [5], Babonneau Nathalie [6], Bayle Christophe [2], Beckler J. [7], Bessette Sandrine [5], Bombled B. [1], Bourgeois S. [8], Brandily Christophe [2], Caprais Jean-Claude [2], Cathalot Cecile [1], Charlier K. [9], Corvaisier R. [10], Croguennec Claire [4], Cruaud Perrine [5], Decker Carole [2], Droz L. [6], Gayet Nicolas [2], Godfroy Anne [5], Hourdez S. [11], Le Bruchec J. [2], Le Saout J. [4], Lesaout M. [6], Lesongeur Francoise, Martinez P. [5], Mejanelle L. [9], Michalopoulos P. [8], Mouchel Olivier [2, 12], Noel Philippe [2], Pastor Lucie [2], Picot M. [6], Pignet Patricia [5], Pozzato L. [1], Pruski A.M. [8], Rabiller Manuella [2], Raimonet M. [10], Ragueneau O. [10], Reyss J.L. [1], Rodier Philippe [2], Ruesch Blandine [4], Ruffine Livio [4], Savignac F. [3], Senyarich C. [8], Schnyder J. [3], Sen Arunima [2], Stetten E. [3], Sun Ming Yi [13], Taillefert M. [7], Teixeira S. [14], Tisnerat-Laborde N. [1], Toffin Laurent [5], Tourolle Julie [2], Toussaint F. [1], Vétion G. [8], Jouanneau J.M. [9], Bez M. [15]

[1] Laboratoire des Sciences du Climat et de l'Environnement, UMR CEA-CNRS-UVSQ 8212 et IPSL, Université Paris-Saclay, Avenue de la Terrasse, 91190 Gif sur Yvette, France
[2] IFREMER Centre Bretagne, Institut Carnot Ifremer-EDROME- Laboratoire Environnement Profond, (REM-EEP-LEP), 29280 Plouzané, France
[3] Institut des Sciences de la Terre de Paris, Sorbonne-Universités, UMR UPMC-CNRS 7193, case 117, 4 place Jussieu, 75252 Paris Cedex 05, France
[4] Unité de Recherche Géosciences Marines, Département REM, IFREMER, 29280 Plouzané, France
[5] Laboratoire de Microbiologie des Environnements Extrêmes, UMR IFREMER-UBO-CNRS 6197, Technopôle Brest Iroise, Plouzané, France
[6] Laboratoire Domaines Océaniques, UMR UBO-CNRS6538, Institut Universitaire Européen de la Mer, 29280 Plouzané, France
[7] School of Earth and Atmospheric Sciences, Georgia Institute of Technology, 311 Ferst Dr., Atlanta, GA 30332, USA
[8] Laboratoire d'Ecogéochimie des Environnements benthiques, Sorbonne Universités, UMR UPMC-CNRS 8222, Observatoire Océanologique, Banyuls-sur-Mer, France
[9] Environnements et Paléoenvironnements Océaniques et Continentaux, Université de Bordeaux, UMR 5805, Allée Geoffroy St Hilaire, 33615 Pessac Cedex, France
[10] Laboratoire des sciences de l'Environnement Marin, UMR UBO-CNRS, Institut Universitaire Européen de la Mer, 29280 Plouzané, France
[11] Equipe Ecophysiologie Adaptation et Evolution Moleculaires, Station Biologique de Roscoff, UMR UPMC-CNRS 7144, 29680 Roscoff, France
[12] Hellenic Centre for Marine Research, P.O. Box 712, P.C. 19013 Anavyssos Attiki, Greece
[13] Department of Marine Sciences, University of Georgia Athens, GA 30602, USA
[14] Centre of Marine Sciences, CIMAR, University of Algarve, Campus of Gambelas, 8005-139 Faro, Portugal
[15] Total, Centre Scientifique et Technique Jean Feger, Avenue Larribau, 64018 Pau, France

* Corresponding author : C. Rabouille, email address : rabouill@lsce.ipsl.fr

Abstract :

The presently active region of the Congo deep-sea fan (around 330 000 km2), called the terminal lobes or lobe complex, covers an area of 2500 km2 at 4700–5100 m water depth and 750–800 km offshore. It is a unique sedimentary area in the world ocean fed by a submarine canyon and a channel-levee system which presently deliver large amounts of organic carbon originating from the Congo River by turbidity currents. This particularity is due to the deep incision of the shelf by the Congo canyon, up to 30 km into the estuary, which funnels the Congo River sediments into the deep-sea. The connection between the river and the canyon is unique for major world rivers. In 2011, two cruises (WACS leg 2 and Congolobe) were conducted to simultaneously investigate the geology, organic and inorganic geochemistry, and micro- and macro-biology of the terminal lobes of the Congo deep-sea fan. Using this multidisciplinary approach, the morpho-sedimentary features of the lobes were characterized along with the origin and reactivity of organic matter, the recycling and burial of biogenic compounds, the diversity and function of bacterial and archaeal communities within the sediment, and the biodiversity and functioning of the faunal assemblages on the seafloor. Six different sites were selected for this study: Four distributed along the active channel from the lobe complex entrance to the outer rim of the sediment deposition zone, and two positioned cross-axis and at increasing distance from the active channel, thus providing a gradient in turbidite particle delivery and sediment age.

This paper aims to provide the general context of this multidisciplinary study. It describes the general features of the site and the overall sampling strategy and provides the initial habitat observations to guide the other in-depth investigations presented in this special issue. Detailed bathymetry of each sampling site using 0.1 m to 1 m resolution multibeam obtained with a remotely operated vehicle (ROV) shows progressive widening and smoothing of the channel-levees with increasing depth and reveals a complex morphology with channel bifurcations, erosional features and massive deposits. Dense ecosystems surveyed in the study area gather high density clusters of two large-sized species of symbiotic Vesicomyidae bivalves and microbial mats. These assemblages, which are rarely observed in sedimentary zones, resemble those based on chemosynthesis at cold-seep sites, such as the active pockmarks encountered along the Congo margin, and share with these sites the dominant vesicomyid species Christineconcha regab. Sedimentation rates estimated in the lobe complex range between 0.5 and 10 cm yr−1, which is 2-3 orders of magnitude higher than values generally encountered at abyssal depths. The bathymetry, faunal assemblages and sedimentation rates make the Congo lobe complex a highly peculiar deep-sea habitat driven by high inputs of terrigenous material delivered by the Congo channel-levee system.

Keywords : Chemosynthetic habitats, Congo deep-sea fan, Fine sediment, Sedimentation rate, Seafloor morphology, Turbidite, Vesicomyidae

1. Introduction

Rivers deliver most of the ~500 Tg y^{-1} (500 10^{12}g y^{-1}) of organic carbon globally exported from land to the ocean (Spitzy and Ittekot, 1991). They also carry large amounts of nutrients which promote large primary production (Jahnke, 2010) and generate a mix of autochthonous marine organic carbon and terrestrial carbon in the coastal ocean (Dagg et al., 2004; McKee et al., 2004). Therefore, continental margins, which represent a crucial link between land and ocean domains, have long been recognized as dynamic reservoirs in the global carbon cycle (Andersson and Mackenzie, 2004; Degens et al., 1991; Liu et al., 2010; Rabouille et al., 2001; Spitzy and Ittekot, 1991; Schlünz and Schneider, 2000; Ver et al., 1999; Walsh, 1988; Wollast, 1993, 1998).

Continental margins present a variety of habitat-forming morphological features such as canyons and seamounts, and host oxygen minimum zones, cold methane seeps, coral and sponge reefs created by the interactions of several driving forces including water properties and dynamics, terrestrial inputs, sediment diagenesis and tectonic activity (Menot et al. 2010; Levin and Sibuet 2012). These habitats display high regional biodiversity under significant threat that needs to be further studied and preserved (Levin and Le Bris, 2015). Cold seeps represent one of the main biodiversity hotspots of continental margins. There, benthic productivity, dominated by chemo-autotrophic fauna and bacterial mats, is stimulated by methane-rich fluids seeping at the sediment surface (Sibuet and Olu, 1998; Sibuet and Vangriesheim, 2009). Inputs of organic matter such as whale carcasses (Smith et al. 1989) or sunken woods (Distel et al. 2000) also sustain chemosynthesis in the deep-sea. Besides these peculiar environments, chemosynthetic fauna in sediment accumulation areas of continental margins has been described only once in relation with large particulate matter deposition in the Laurentian fan (Mayer et al., 1988).

Submarine canyons play a critical role in the transfer of particulate material from the coastal ocean to the open ocean because they rapidly channel particles to the deep-sea (Canals et al., 2006; Heussner et al., 2006; Monaco et al., 1990; Sanchez-Vidal et al., 2012). As a result, large quantities of

organic matter of terrestrial and marine origin (Goni et al., 1997; Hedges et al., 1997), and also recycled old organic matter (Tesi et al., 2010), are transferred from the continental shelf to the deep-sea by turbidity currents (Khripounoff et al., 2006; Vangriesheim et al., 2009a) or cascading dense water flows (Canals et al., 2006; Ulses et al., 2008). The supply of organic matter is able to maintain high densities and diversities of benthic organisms in at least some deep continental margins (Levin and Sibuet, 2012), such as in the Congo/Angola margin near the Congo canyon (Galeron et al., 2009; Van Gaever et al., 2009).

In this context, the Congo canyon and deep-sea fan are particularly interesting as they provide the sole example of a major river directly connected to a large canyon (Babonneau et al., 2002; Milliman, 1991). In this system, a massive and direct transfer of particles into the canyon and the channel-levees of the deep-sea fan is driven by strong turbidity currents (Savoye et al., 2000, 2009). Preliminary observations from two remotely operated vehicle (ROV) dives in the investigated area during the ZaiangoROV cruise (Savoye and Ondreas, 2000) detected the presence of microbial mats and vesicomyid bivalves (unpubl. data). They resemble the biological communities associated to cold seeps (Nelson et al., 1989; Sibuet and Olu, 1998), especially those located on the continental slope pockmarks near the Congo canyon (Olu-Le Roy et al., 2007).

This paper reports the observation methodologies and sampling effort conducted during two cruises devoted to the multidisciplinary investigation of the terminal lobes of the Congo deep-sea fan in 2011 and 2012: WACS (Olu, 2011) and Congolobe (Rabouille, 2011). It presents the first high-resolution bathymetric maps of some portions of the lobes obtained using ROV-based multibeam bathymetry and introduces sampling locations. The biological habitats sampled during the WACS and Congolobe cruises are described with a few photographs. Finally, sedimentation rates measured in this complex and heterogeneous system are reported and discussed.

2. Background information

The Congo River is the second largest river on Earth by its freshwater discharge (1250 km^3/yr) and by its drainage basin area (3.7 10^6 km^2; Milliman, 1991) with limited seasonal variation of flow because of the location of its drainage basin on both side of the Equator (Laraque et al. 2009). Since the Oligocene, the Congo fan, one of the biggest deep-sea fans in the world, has developed on the West African margin, fed by particulate inputs from the Congo River. The Late Pleistocene deposits are still visible on the seabed morphology as an intricate network of about 90 highly sinuous channel-levees terminated by lobe-shaped deposits characterized by poorly channelized morphologies and called terminal lobes or lobe complexes (Droz et al. 2003; Marsset et al. 2009, Picot et al. 2015). The channel network has developed by successive phases of channel bifurcation and abandonment and all the channel-levees but one, the youngest one, are fossil. This latter channel-levee is connected to the Congo canyon and extends 750 km across the continental slope and rise and the abyssal plain (Babonneau et al. 2002). Present and Holocene turbiditic activity along the canyon and channel-levee has been demonstrated by cable breaks (Heezen et al. 1964), by sediment trap studies (Khripounoff et al., 2003) and by dating of turbidites (Migeon et al. 2004; Dennielou, 2002).

The extremity of this active channel-levee, at 4750 m water depth (Babonneau et al. 2002) is characterized by the gradual vanishing of the channel and the development of lobe-shaped sedimentary bodies that constitute what we call the lobe complex. Based on bathymetry and seismic data, five adjacent and partly stacked lobes have been identified (Savoye et al., 2000; Babonneau, 2002; Bonnel, 2005). Each lobe have developed at the termination of distributary channels and the 5 successive lobe have developed and migrated 50 km south-westward from channel-levee by successive avulsions of the feeding channel (Dennielou et al. this issue). Based on the morphological features and structure of the lobes it was postulated that the age of the lobes decreases downstream (Savoye et al., 2000; Babonneau, 2002; Bonnel, 2005; Dennielou et al. this issue) and, therefore, the lobes have been labelled from 1 to 5 in a structural and chronological order. Based on excess ^{210}Pb

analyses on the lobes and radiocarbon dating on the levees (Dennielou, 2002; Savoye et al., 2009), it was proposed that the development of the lobe complex started during the Holocene. The age of this onset was refined to 4 ka BP by Picot (2015).

There is another, older, lobe complex emplaced to the north of the recent lobe complex. The feeding channel is connected to active channel-levee but was abandoned after the avulsion of the active channel to the south to feed the active lobe complex. This abandoned lobe complex is called the northern lobe complex and probably also developed during the Holocene, but between 6 and 4 ka BP (Picot 2015).

Sediment cores collected all over the lobe complex show dominantly muddy turbidites with sand confined inside the distributary channels (Babonneau, 2002; Bonnel, 2005). In this particular area, deposits represent a mix of particles discharged by the canyon, composed of Congo River and shelf particles with little proportion of biogenic material settling from the surrounding water column (Baudin et al. 2009; Stetten et al. 2015; Treignier et al., 2006). The organic carbon discharge from the Congo River is $2x10^{12}$ g OC/yr (Coynel et al., 2005) with a clear signature from soils (Spencer et al., 2012). This high organic discharge induces an intense biogeochemical recycling of biogenic particles (organic carbon-OC, biogenic silica-bSi) in the Lobe region due to the funnelling of the particle flux into the canyon down to the terminal lobe zone with very little lateral export to the levees mid-slope down to 4000 m (Rabouille et al., 2009 ; Ragueneau et al., 2009). Background oceanographic information in the canyon area can be found in Vangriesheim et al. (2009) while chemical, biogeochemical and biological data in the Angola slope area and near canyon pockmark zone are reported in the Deep-Sea Research II volume on Biozaire (2009, Vol. 56).

3. Material and methods

3.1 Cruise description and sampling strategy

In 2011, two cruises were conducted on the RV Pourquoi Pas?: the second leg of the WACS cruise in February 2011 (10 days) and the Congolobe cruise between mid-December 2011 and mid-January 2012 (30 days). During these cruises, two types of operation were performed: ship board operations consisting of coring and deployment of *in situ* instruments and sampler and ROV-based operations consisting in bathymetry, seafloor observations, sampling and *in situ* measurement (Table 1).

Six sites were chosen among the different morpho-sedimentary environments of the lobe complex in order to span areas of various turbiditic activity (Fig. 1). Sites A, F and C are located along the active feeding channel from upstream to downstream. Site A is located on the channel-levee at the entry of the lobe complex. Site F is located 40 km downstream of site A. Site C is located 25 km downstream from site F, at the termination of the feeding channel at the entrance of the youngest lobe (number 5). Site D is located at the outer rim of the youngest lobe n°5 at the most distal part of the lobe complex. Site B is located on the main body of lobe number 3, 22 km WNW of site A (Fig. 1) and 10 km north of the feeding channel. Site E is located on the abandoned northern lobe complex, 45 km north of the feeding channel of the active lobe complex.

3.2 Ship-operated tools

As described in Table 1, two types of cores were collected: multicores (MTB) which preserve the sediment-water interface and Calypso cores (CS) which allow coring through geological strata (5-25 meters). Free-falling instruments were also deployed during the cruises: (i) a respirometer which allow the measurement of benthic fluxes over 24 hours (RAP, Khripounoff et al., 2006) carried 3 benthic chambers and a microprofiler as described in Rabouille et al. (2009) which deployment was monitored with a video-camera to determine the penetration depth of the chambers in the sediments and (ii) a mooring line with one sediment trap to measure particle flux and a ADCP current

meter which was deployed during the WACS cruise in February 2011 and recovered during the Congolobe cruise in December 2011 (Table 1). The sediment trap was positioned 45 meters above bottom (m.a.b) and the current meter positioned 35 m.a.b. (Khripounoff et al., 2003). The sediment trap had an opening of 1 m^2 and contains 24 collecting cups programmed for 15 days rotation. The cups were filled with formaldehyde to prevent bacterial activity and preserve trapped particles (Vangriesheim et al., 2009a).

3.3 ROV-operated tools

Ifremer's ROV Victor 6000 is an instrumented deep water, remote-controlled system able to perform high-resolution bathymetry, high quality optical imagery, operate underwater instruments and perform scientific sampling (http://flotte.ifremer.fr/fleet/Presentation-of-the-fleet/Underwater-188 systems/VICTOR-6000).

3.3.1 High-resolution bathymetry

During the Congolobe cruise, the ROV Victor 6000 was equipped with a high-resolution multibeam echo-sounder (Simeoni et al., 2007) and a long-range black and white camera (Table 1).

At each site, data acquisitions for bathymetry were performed at a speed of about 0.4 m s^{-1}, under two configurations:

- A survey was conducted at an altitude of 60 m, providing a swath width of about 200 m. To improve the data quality, and insure good overlap of multi-beam data, profiles were separated by 180 m. At each site, an orthogonal profile was also acquired to ensure an efficient geographical fit between parallel profiles. Using these data, high-resolution bathymetric maps were compiled with a depth resolution of about 1 to 2 m (<5% altitude)

- Additional transects were performed at each site at an altitude of 8 m to simultaneously survey fauna clusters using an OTUS camera with 8 meters wide images and acquire further bathymetric data. With this configuration, the bathymetric vertical resolution increased up to 0.2 m. Details of data collection on each site are given in Table 2.

A total of about 150 km of high-quality bathymetric and acoustic backscatter data in three deep-waters (5000 m) study sites were acquired. The bathymetric and backscatter data were processed on-board with CARAIBES software of Ifremer (http://flotte.ifremer.fr/fleet/Presentation-of-the-fleet/On-board-software/CARAIBES) and a 1 m DTM was provided in order to guide the survey for biological habitats and their sampling. Bathymetric maps presented in this paper have been reprocessed on-shore.

3.3.2 *In situ* habitat observation and sampling

Sites for investigation of the chemosynthetic habitats (e.g. microbial mats, vesicomyid bivalves clusters) were selected from the intensive OTUS camera surveys described above, guided by topographic structures together with acoustic backscattering. Faunal assemblages spotted by the OTUS Camera were further observed at 3 meters altitude to improve image resolution with the ROV HD-colour video cameras.

Intensive sampling was performed on a selection of densely populated habitats (bacterial mats, bivalves, black sediment patches. Typically for each habitat, 8-16 push cores (CT) with a diameter of 8 cm were collected in order to analyse geochemical and microbiological parameters, 3 to 4 blade corers (GCL 300 cm^2 or PCL 150 cm^2) were taken for macrofaunal and megafaunal analyses and several net samples were obtained to collect bivalves. Bottom water approximately 5 cm above the sediment-water interface was also collected near the investigated habitats using a ROV-operated tube and a water collection system (PEP, Olu-Le Roy et al., 2007).

In addition, ROV movable benthic incubation chambers (CALMAR; Caprais et al., 2010) were deployed in these habitats and in surrounding sediments, and *in situ* bivalve incubations were conducted with these chambers (Khripounoff et al., 2015). Finally, the ROV-movable autonomous microprofiler (Deep Micro Profiler System, DMPS) equipped with a Unisense microprofiler (as described in Rabouille et al., 2009) carrying oxygen, pH, and sulfide microelectrodes was deployed from the ship and handled by the ROV using floats to reduce its weight in water. The deployments

were achieved on selected habitats (mostly bacterial mats and black sediment patches), as micro-electrode profilers are not suitable for working on hard substrates such as shells.

All ROV deployments were associated with a set of photographs that documented the exact location of the sampling and *in situ* measurement. Some of these photographs are presented in this paper but the data collected in the habitats will be presented in separate publications of this special issue.

3.4 Radionuclide measurements and sedimentation rate calculations

During the Congolobe cruise, sediment samples from the multicorer were vertically sliced at 0.5 and 1 cm intervals and dried at 100 °C for two days on board. Calypso cores were sub-sampled in the laboratory: 1 cm layers were collected down to 1 to 6 meters down-core upon requirements, and dried at 100°C. Before measurements, samples were gently ground and sealed for non-destructive gamma spectrometry in polyethylene tubes as described previously in Rabouille et al. (2009). The activities of ^{234}Th, ^{228}Th, ^{210}Pb, ^{226}Ra, ^{228}Ra and ^{137}Cs were measured on 2-6 g of dried sediment using three low-background high-efficiency well-type (215, 430, 980 cm^3) Ge gamma detectors and calibrated with several IAEA standards: RGU-1, RgTh-1, IAEA 447. These measurements were conducted at the Laboratoire Souterrain de Modane (LSM) in the French Alps which is protected from cosmic radiations by 1700 m of rocks overburden (Reyss et al., 1995; Cazala et al., 2003). We report $^{210}Pb_{xs}$ activity, i.e. the difference between ^{210}Pb and ^{226}Ra activities.

Other samples collected during the Zaiango cruises in 1998 (Savoye et al., 1998; Cochonat et al., 1998) using piston cores (KZAI) and their trigger gravity cores (KPZAI) were analyzed for ^{210}Pb and ^{226}Ra by high-resolution gamma spectrometry at EPOC (Dennielou, 2002) in 2000. Some of these samples were re-analyzed at the LSM using the above technique to cross-calibrate the present data and simultaneously provide ^{137}Cs measurements. Activities of $^{210}Pb_{xs}$ measured in 2015 were recalculated in year 2000 to compare the present data to the initial data.

Concerning the calculation of sedimentation rate from on $^{210}Pb_{xs}$ distribution, we used the Constant Flux-Constant Sedimentation rate model (CFCS, Appleby et al., 2001) for depths below 10 cm in a

preliminary approach. This choice was made although deposits represent a mix of riverine and marine particles probably including particles eroded along the canyon and channel and because of the temporal discontinuity of the fluxes from turbidity currents. Indeed, as the recurrence of turbidity currents in the canyon (≈2 years, Heezen et al., 1964) is much smaller than the half-life of ^{210}Pb and as the turbidity flux is much larger than the vertical hemipelagic flux of particles (Rabouille et al., 2009), a constant flux over periods longer than a decade can be assumed as a working hypothesis.

^{137}Cs can also be used to estimate recent sedimentation rates, as this artificial radionuclide was produced by the atmospheric nuclear weapon tests and spread in the environment during the sixties with a maximum production in 1963. Therefore, it is a fair temporal marker and sediments containing ^{137}Cs are considered to have settled after 1963. Using this interpretation, maximum sedimentation rates were estimated based on the maximum depth of ^{137}Cs penetration in the core divided by the time elapsed since 1963, *i.e*. 49 years for Congolobe in 2012 and 35 years for Zaiango in 1998. Bioturbation entrains particle-bound Cs to the bottom of the sediment mixed layer (Berner, 1980), which averages 10 cm depth (Boudreau, 1998). This generates large uncertainties in sedimentation rate calculations when applied to slowly accumulating sediments of abyssal plains, where bioturbation is much more efficient than burial in transporting particles to depth. In rapidly accumulating sediments of the Congo lobe complex, however, this method is much less biased by bioturbation.

4. Morphological features of the study areas and shipboard sampling

- **Site A**

The high-resolution bathymetry covers about 3.8 km^2 and reveals contrasting morphologies despite the low amplitude (45 m) in the water depth fluctuations between 4745 and 4790 m. The most visible features are two channels (Fig. 2). The southern channel is 45 m deep and around 1400 m

wide and shows a 30° bend to the south. It is the prolongation of the active channel-levee of the Congo fan that feeds the recent lobe complex. The channel floor is rather flat and widens westward from 830 m to 935 m. The channel flanks are asymmetrical with a steep (up to 60°) northern flank and a gentle (mean slope < 5°) southern flank. The southern flank shows several headscars with adjacent sediment blocks. Outside the channel, mostly flat or gently sloping areas are interpreted as levees. The northern channel is related to lobe number 3. It is 25 m deep and 1000 m wide with a central 200 m wide inner channel. It has a faint morphology possibly because it is partly buried by spill over sediment from the southern channel (Fig. 1) but may also serve as a conduit for these sediments to lobe 3. It is therefore less active than the southern channel. The flanks show evidences of widespread slides towards the channel axis providing a highly hummocky aspect.

At this site, two Calypso piston cores were collected (Fig. 2 and Table 3). Core CoL-A-CS01 was collected at 4755 m water depth on the northern (right-hand) levee of the southern channel. Core CoL-A-CS02 was collected at 4764 m water depth on the southern and internal gentle flank of the southern (left-hand) channel and particularly on a slump scar, where clusters of fauna were discovered. The RAP was deployed on the northern levee (CoL-A-RAP1 and WACS-A-RAP3) together with the multicorer to obtain sediment samples (WACS-A-MTB3 and CoL-A-MTB2&13). Another multicorer (Col-A-MTB3) was obtained in the channel, near the south flank and fauna clusters (bivalves and microbial mats, marker CoL2), which were investigated during dives 483-484 (Markers CoL1 and CoL2). Finally, a mooring line with a sediment trap and a current-meter (WACS-A-PPART3) was deployed in the southern active channel at 45 meters above bottom (Fig. 2).

- **Site B**

High-resolution bathymetry could not be acquired at site B, but the low-resolution bathymetric map (50 m grid, Fig. 3) reveals a small sinuous channel, with few meters high levees, that is connected to the northern channel of site A. This channel feeds lobe number 3, with much less transport than the active southern channel (see site A section above).

At this site, one Calypso piston core (CoL-B-CS07) and a multicore (CoL-B-MTB12) were collected at 4822 m water depth on the southern (left-hand) of the lobe 3 feeding channel (Fig. 3 and Table 3). Piston cores KZAI-09 is located further downstream where the lobe 3 feeding channel has vanished. Piston core KZAI-12 is located on the northern (right-hand) levee, further upstream of the channel, at midway between the lobe 3 feeding channel and the active channel coming from site A (Fig. 1). The respirometer (CoL-B-RAP5) was deployed 500 meters east on the same levee.

- **Site F**

The high-resolution bathymetry reveals a 2.5 km wide 45 m deep NNE-SSW channel that slightly widens downstream and is the continuation of the active channel described on site A. It comprises a shallower and narrower inner channel that is 15 m deep and 350 m wide to the NNE and that also widens to reach 650 m width to the SSW. The morphology of both flanks appears strongly indented and hummocky with numerous flat depressions, scarps and blocks.

A Calypso core (COL-F-CS03) was sampled at 4886 m water depth as a reference for undisturbed levee sediments on the western (right-hand) flank of the channel. Multicore sampling (CoL-F-MTB 4-5-7) was conducted at the same location of the Calypso core to investigate organic matter recycling on the levees. The respirometer was deployed on the same levee (CoL-F-RAP2, Table 3).

- **Site C**

The high-resolution bathymetry reveals a shallow (11 m deep) channel widening downstream of more than 5000 meters. The channel floor is rather flat and is flanked by poorly developed hummocky levees. It is interpreted as the most recent deposition zone at the end of the channel.

Four Calypso cores were collected at this site: Core CoL-C-CS04 was obtained from the northern levee at 4949 m water depth, and cores CoL-C-CS05, CoL-C-CS06, and WACS-CS07 were sampled in the channel at 4954 m water depth (Fig. 5). Two additional piston cores had been collected 12 km upstream at the entrance of lobe number 5 during Zaiango cruise: KZAI07 located in the active feeding channel and KZAI08 located on the northern levee (Fig. 1). Multicores were also collected on

the northern levee (Col-C-MTB-6-8-9) and within the channel near microbial mats and dense vesicomyid habitats near marker CoL9 (Col-C-MTB10-11 and WACS-C-MTB4-5-6). The respirometer was deployed twice in the channel (Col-C-RAP3 and WACS-C-RAP4) (Fig. 5 and Table 3).

- **Site D**

Site D (Fig. 6) was placed at the outer rim of lobe number 5 (Fig. 1) where sidescan backscatter showed evidences of morphologies, probably related to recent, turbidity deposits (Bonnel, 2005). This site, surveyed during the WACS cruise in February 2011, is located 18 km southwest of site C, in water depths around 5000 m. The area is gently sloping south-westwards (around 0.2°). Note that the deep channel located to the north of site D is not related to the modern lobe complex: it was abandoned long time before the onset of the present lobe complex (Picot et al., 2016). The channel morphology is still visible due to the small thickness of the post-abandonment sedimentary cover.

One Calypso core (WACS-D-CS06) was collected at 4996 meters depth. A ROV dive (PL 438) was performed at the outer edge of the deposition zone, but no chemosynthetic habitat or fauna indicative of sulfide-rich sediments were found, and therefore are not discussed in the next section. Push cores were collected during this dive near marker W13.

- **Site E**

Site E (Fig. 7) is located on the former feeding channel at the entrance of the northern lobe complex, approximately 45 km to the north of site A. The bathymetric map (low resolution only) reveals a wide bulge with a faint channel-levee, which morphology indicates an abandoned system.

One multicore (CoL-E-MTB14) was sampled at the same location as the ROV deployment. The ROV dive PL 494 investigated the channel and the levees at the approximate water depth of 4750 m. No habitat typical of reduced conditions was found in this area and sponges of different morphologies and holothurians dominate.

5. Dense habitat description

A number of different habitats resembling chemosynthesis-based cold seep ecosystems (bacterial mats, reduced sediments, vesicomyid clusters) were observed and sampled during the ROV dives at sites A, B, C, and F. These habitats were not found at sites D and E. For some of these habitats, we used physical markers: WXX for markers deployed during WACS, or CoLXX for those used during Congolobe.

Site A

During the Congolobe cruise, sampling dives PL483 and 484 were conducted along the southern gentle bank of the active channel shown in Figure 2 where large concentrations of bivalves belonging to the Vesicomyidae family were found associated with black reduced sediment and sometimes microbial mats (Fig. 8a). This first sampling site gathered several small clusters of very densely packed vesicomyids (marker CoL2, Fig. 2). They were dominated by the species *Christineconcha regab*, (Cosel and Olu, 2009; Krylova and Cosel, 2011), which also dominated the vesicomyid population of the Regab pockmark, located at 3200 m depth along the Congo margin (Olu-Le Roy et al., 2007). Another species, *Abyssogena southwardae* (Krylova et al., 2010), has also been identified and sampled at this site in a much lower density than C. *regab*. This species is assumed to be amphi-Atlantic as it is also known from the Mid-Atlantic Ridge hydrothermal vents, Barbados prism and Florida seeps (Teixeira et al., 2013). Vesicomyids and the associated macrofauna were sampled with blade corers (GCL), while sediments were collected using push-corer (CT) for microbial community analysis, and biogeochemical investigations of sediments and pore waters. A benthic chamber (CALMAR) was deployed on the habitats and overlying water was sampled by PEP above the vesicomyids. Large size tubicolous polychaetes identified from samples as belonging to the Ampharetidae family were abundant among the bivalves. Another vesicomyid patch located near

marker W11 was studied during PL435 of the WACS cruise (Figs. 2 and 8b). This patch was located on the northern levee of the active channel (Fig. 2), and CTs and GCLs were collected together with a CALMAR measurement over the bivalves.

A patch of black sediment with white filaments in its periphery was observed near marker CoL1 and was called “King Kong” (Fig. 8c). Such patches are common features of cold seeps and typically exhibit sulfide-rich and oxygen-poor porewaters near the surface of the sediment. The white material generally consists of microbial filaments of large sulfide-oxidizing bacteria, such as *Beggiatoa* sp., that is characteristics of the most sulfidic habitats at cold seeps (Niemann et al., 2006; Pop Ristova et al., 2012). Only a few empty vesicomyid shells were observed lying on the sediment in the patch, while some seem to be living in the near vicinity, half buried in the sediment. Tubes of polychaetes were also observed in the patch, but have not been sampled. A limited set of CTs was collected on this reduced sediment patch.

Site F

ROV dive PL486 (Fig. 5) explored depressions on the western flank of the channel where the large inner channel divides and presents indented flanks with scars and blocks (see description above). Numerous small bacterial mats with sparse vesicomyid patches were observed during this dive. At this site near marker CoL3, low densities of vesicomyids with some dead white shells and microbial mats were located along the flanks of a small relief (Fig. 9). Small patches of black sediment were visible under the white microbial filaments and within the tracks made by the bivalves. Both *C. regab* and *A. southwardae* species, were collected at this site though *C. regab* dominated. The sample size was too low (total of 18 specimens) to be conclusive on the relative proportion of each species. Most bivalves found in these black patches were alive though a few empty shells were observed between patches. These bivalves were sampled with underlying sediments using blade corers (GCL and CL). Pushcores were collected and analyzed for microbial and geochemical analysis while CALMAR was deployed on a small vesicomyid spot near marker CoL3.

Site B

ROV dive PL 492 explored the less active northern channel bottom of site B and its northern and southern levees, located 10km away from the active channel (Fig. 3). Sparse vesicomyids were observed together with decimeter-scale reduced sediments patches (Fig. 10). The grainy texture of the sediment is indicative of degraded bacterial mats which form thin crusts at the sediment surface (Vigneron et al., 2013). Vesicomyid patches were dominated by dead shells which cover a large area in this zone. Interestingly, *A. southwardae* was the most abundant species at site B, as the otherwise dominant species *C. regab* was present in minority at this site. Most samples (CT, GCL, nets) were collected near marker CoL11 in one of the typical vesicomyid sparse habitat (Fig. 10). Four CT's (9-12) were collected near marker CoL12 (Fig. 10).

Site C

Five ROV dives were conducted in the southern, central and northern part of the channel at site C (Fig. 5). The first dive (WACS-PL 436) explored the southern levee and the southern part of the channel, where CT samples were collected from a bacterial mat in the vicinity of marker W12 (Fig. 11a). All other dives (PL 437-489-490-491) were devoted to sample other chemosynthetic habitats and reduced sediments near markers CoL4, W15-CoL9 and CoL8 (Figs. 5 and 11). Bacterial mats, hypothesized to be constituted by sulfide oxidizing bacteria, associated with black sediment patches (Fig. 11b) have also been observed during PL489-490 at several other places at site C in the northern part near CoL4 (Fig. 5). Sampling was performed using blade and push-corers for fauna, microbes and chemical characterization. The sediment consisted of a thin crust on the top overlying an extremely soft bottom. This sediment was so soft that a blade corer (GCL3, size 50 cm) was lost, buried during deployment, and CALMAR chambers occasionally flipped upon deployment. The underlying sediment was reduced as observed from the black colour of the sediment when corers were retrieved (not shown).

Figure 11c shows a black patch of reduced sediment with a few empty shells of vesicomyids near marker CoL8 (called “Black ogre”). The composition of the black layer on the top still needs to be characterized as it was difficult to keep the thin interface sediment layer intact during sampling by ROV-operated push-corers or blade corers. A microprofile series was performed using the autonomous microprofiler (CoL-DMPS 3) during dive PL 490 on nearby reduced sediments similar to the one displayed on Fig. 11c.

Dense habitats with vesicomyid bivalves were observed in two patches, respectively called « the heart » (Fig. 11d) and “the mouth” (Fig. 11e), during both WACS and Congolobe cruises (PL437 and PL491). These patches revealed the most complex organization that has been observed so far. Although the center of the black sediment, except for a few empty shells, was devoid of bivalves in both patches, the periphery of the patches was densely colonized by bivalves. Among them, Ampharetidae polychaete tubes have been sampled and are visible on images. A few Zoarcidae fishes, common at cold seeps, were also observed around the aggregate. In “the heart”, some smaller vesicomyid patches were visible, a few decimeters around the main cluster. *C. regab* largely dominated the specimen sampled, compared to *A. southwardae* that seems more rare in these patches. Blade and push-cores, nets, and overlying water were collected at both sites. A special sampling scheme was devised with samples taken inside and outside the patch for contrast studies. In situ CALMAR benthic chambers were deployed on both patches together with the microprofiler at “the mouth” (W15), where O2, pH and dissolved sulfide depth microprofiles were successfully obtained (W-C-DMPS4).

Proposed functioning of the observed habitats and comparison to cold-seeps

The habitats observed at these four sites appear similar to those associated with cold seeps where mats of giant filamentous sulfide-oxidizing bacteria are generally associated with low porewater levels of dissolved oxygen and high concentrations or fluxes of dissolved sulfides (Nelson et al., 1989; Niemann et al., 2006) and where large vesicomyid bivalves, a family known to carry sulfide-oxidizing

symbionts, may settle and form colonies in the deep-sea (Fiala-Médioni and Felbeck, 1990; Sibuet and Olu, 1998). These biological communities indicate the presence of hydrogen sulfide which can be produced in anoxic, organic-rich sediments by sulphate reduction or anaerobic oxidation of methane (AOM) coupled to sulphate-reduction (Boetius et al., 2000). The dominant pathway for sulfide production and methanogenesis in the sediments of the Congo deep-sea fan remains to be elucidated, but could be related to the large inputs of organic carbon from the canyon which may drive anaerobic decomposition of organic matter by sulphate-reducing and methanogenic bacteria and archaea. This was already observed in organic-rich environments, near whale carcasses (Smith et al., 1989) or at one canyon outlet near the Laurentian fan (Mayer et al., 1988). The observed communities resemble the chemosynthetic communities associated with active methane seeps in a large pockmark area discovered in the vicinity of the Congo canyon at 3150 m depth (Ondréas et al., 2005; Olu-Le Roy et al., 2007; Pop Ristova et al., 2012). Chemosynthetic organisms have also been observed sporadically along the Congo main channel flanks between 3000 m and 4000 m depth (Olu et al., unpubl.).

6. $^{210}Pb_{xs}$ and ^{137}Cs profiles and sedimentation rates in the different zones

Depth profiles of excess ^{210}Pb ($^{210}Pb_{xs}$, $T_{1/2}$ =22.3 yr) and ^{137}Cs in the sediment cores collected with the multicorer are presented in Fig. 12. All cores, except cores obtained at site E and KZAI12, showed ^{137}Cs and $^{210}Pb_{xs}$ in the upper sediments. The sediment-water interface was well preserved by the multicorer, and high activities of short half-life radionuclides ^{234}Th ($T_{1/2}$ = 24.1d) and ^{228}Th ($T_{1/2}$ = 1.9yr) (not shown) were found in the 2 top centimeters together with large activities of $^{210}Pb_{xs}$ (>500Bq/kg). This particular layer is affected by deposition, accumulation, erosion, diffusion, early diagenetic, and bioturbation processes before its incorporation in the sedimentary column (Turnewitsch et al., 2008), which explains its different signature compared to the rest of the core. Interestingly, this enriched layer was not observed in piston cores (CS, KZAI) and their associated “pilot” cores (KPZAI), probably indicating a partial loss of the sediment-water interface during this type of coring. As the upper

sediments obtained by Calypso or piston coring display $^{210}Pb_{xs}$ and ^{137}Cs activities that are larger than 1 Bq/kg, it is likely that the loss of sediment was limited to a few centimeters. Therefore, sedimentation rates calculated for the KZAI and KPZAI cores based on ^{137}Cs penetration represent minimum values. The depths of the first layers of the Calypso cores were adjusted using the ^{210}Pb and ^{137}Cs contents of the MTB cores, when collected at the same location. It is noteworthy that $^{210}Pb_{xs}$ did not reach zero at depth, though very low levels (around 10 Bq/kg) were reached in most cores. This issue is either due to the underestimation of ^{226}Ra activity (which is subtracted from raw ^{210}Pb activity to calculate excess) during gamma counting as a result of calibration uncertainties or the upward diffusion of dissolved ^{226}Ra (Cochran, 1985) which creates a background of $^{210}Pb_{xs}$. This slight shift in $^{210}Pb_{xs}$ does not alter significantly the calculation of sedimentation rates, as the slope of the regression of the log-normal plot is shifted by no more than 10%. Cores at site C and KZAI07 showed very large $^{210}Pb_{xs}$ and ^{137}Cs values over meters of sediment. For example, the Col-C-CS06 core displayed a ^{137}Cs penetration over 6 meters, whereas KZAI07 displayed ^{137}Cs activities larger than 1Bq/kg at 90 cm depth. These values lead to sedimentation rates of around 10-22 cm yr^{-1} for Col-C-CS06 and >2.5 cm yr^{-1} for KZAI07 depending on the method (Table 4), which represents an ultra-high sedimentation rate for sediments at 5000 m deep. These extreme sedimentation rates are likely related to the position of this station at the end of the main channel, where fine material accumulates (Bonnel, 2005). At the other sites (A, B, KZAI08, KZAI09), coring was performed on the levees at increasing distance from the main channel. As a result, sedimentation rates are much lower and range between 0.3 and 1 cm yr^{-1} (Table 4). Although the absence of ^{137}Cs in the surface layer of KZAI12 may be indicative of a larger loss of surface sediments during coring, it is unlikely the case as piston coring procedures were similar at each station during the same cruise. The lack of ^{137}Cs in this core could also be due to local erosion as ripples characteristic of mass transfer through resuspension are visible in levee sediments (Dennielou et al., this issue). This process could explain the difference in ^{137}Cs activity between KZAI09 and KZAI12 (Table 3) which were collected in the same lobe and the same levee at 12 km distance. Finally, the MTB core obtained at station E

contained no ^{137}Cs, likely resulting from the low sedimentation rates at this site located outside the active channel (50 km northwards).

With the exception of this station, sedimentation rates recorded in the active lobe zone (Table 4) are much larger than sedimentation rates reported for the Holocene in the area, i.e. 2-8 cm kyr^{-1} in the deep area of the Gulf of Guinea and its abyssal plain (Mollenhauer et al., 2004). The values reported for the active lobes of the Congo deep-sea fan are therefore 100 times larger than values in the abyssal plain in the levees of the present channel and 1000 times larger in the present deposition area (Site C).

7. Synthesis

In the interdisciplinary studies reported in this special issue, *in situ* technologies and ROV sampling operations were combined with conventional multicorer and piston corer sediment sampling during two cruises (WACS and Congolobe) on the youngest lobe complex of the Congo deep-sea fan to characterize their geology, organic and inorganic geochemistry, and micro- and macro-biology. The ROV Victor 6000 was deployed at a depth of around 5000 m to obtain high-resolution bathymetric mapping and habitat imaging, deploy *in situ* instrumentation on the seafloor (micro-electrode profiler, benthic chambers) and collect overlying water, sediment and biological samples using corers, nets, and water sampler.

Combined with previous geological work on the active Congo lobe complex, this dataset sheds light on the functioning of the lobe area. First, the channel is well marked at the entrance of the lobe complex (site A) and becomes wider and smoother downstream, towards its distal end (stations F and C). The channel that was abandoned by the channel avulsion and prograding building processes of the lobes (site B) are still visible on high-resolution bathymetry and may carry part of the secondary turbidity flow that spills over the main active channel. Site C represents the main deposition zone while the most western site D does not presently show signs of large deposition. The

northernmost site E is abandoned, and does not presently receive turbiditic material. Simultaneously, the reported variations in sedimentation rates in the lobe complex can be explained by the morphological differences between the lobe entrance and the lobe terminal deposition zones. The high sedimentation rates found at site C (up to 12-22 cm yr^{-1}) are consistent with channel infill processes inferred from morphological and geological observations. Sedimentation rates on the levees at site A or B are at least one order of magnitude below sedimentation rates in the terminal lobe (site C), yet much higher (i.e. 0.6 to 1 cm yr^{-1}) compared to abyssal sediments, indicative of deposition processes from turbidity currents. Furthermore, sedimentation rates at sites A and B (~1 cm yr^{-1}) agree well with sediment rates recorded in the Amazon deep-sea fan during the glacial period, when the Amazon fan was actively connected to the Amazon River, as is presently the case for the Congo deep-sea fan (Schlunz et al., 1999). In contrast, present time sedimentation rates in the Amazon fan are two orders of magnitude lower (around 5-10 cm kyr^{-1}) than sedimentation rates in the Congo deep-sea fan, as most of the sediments delivered by the Amazon are deposited on the continental shelf while intense turbiditic activity feeds the lobes and maintains large sedimentation rates in the Congo fan. Finally, *in situ* observations and fauna collection revealed dense bivalve populations located in spots associated with bacterial mats and black sediments all along the active channel at site A, F and C. The bivalves belong to the Vesicomyidae family and include the two species *Christinaconcha regab* and *Abyssogena southwardae,* which are symbiotic bivalves previously reported at active cold-seeps and hydrothermal vents. Sparser and smaller vesicomyid communities were observed at site B, located 10 km away from the active channel, compared to sites located near the main channel. The occurrence of these bivalves at site B provides information on the temporal persistence of these assemblages when disconnected from the active channel. Site E, located in a zone which has been disconnected for millennia, revealed no signs of faunal community linked to reduced sediments (bacterial mats or vesicomyids), and rather showed classical deep-sea megafauna such as sparse sponges and holothurians. Overall, the results indicate that these habitats are sustained by large inputs of organic material around the active channel connected to the Congo

canyon, but further analysis is needed to better understand the origin of this gradient and the persistence of these ecosystems through time as well as their relationship to the large-scale geological evolution of the deep-sea fan.

Acknowledgments

We express our deepest gratitude to the captains and crews of the N.O. Pourquoi Pas ? who operated the ship and the equipment during the WACS and Congolobe sea expeditions. We would also like to acknowledge the hard work of the ROV Victor 6000 teams to maintain the submersible over these two cruises. JM. Sinquin and MP. Corre (Ifremer/NSE) trained our personnel (LD, MP, and MLS) to the Caraïbes software to accurately record the position of the geological structures and the habitats in real-time during the cruise. Finally, we would like to thank E. Krylova for her help in identifying vesicomyids, N. Kiriazis for some of the chemical analyses, and C. Berrached and L. Petitjean for preliminary data analyses. Total participated in this research through funding of the ZAIANGO project. We also acknowledge the detailed comments and suggestions from a reviewer which largely improved the paper. This project was funded by ANR Congolobe (ANR Blanc SIMI5-6, n°11 BS56 030), IFREMER (Project "Biodiversité et dynamique des écosystèmes profonds, impacts"), CEA through LSCE (to CR) and by the U.S. National Science Foundation Chemical Oceanography Program (OCE-0831156 to MT).

This is LSCE publication number 5721

References

Andersson, J.A., Mackenzie, F.T., 2004. Shallow-water oceans: a source or sink of atmospheric CO_2? Front. Ecol. Environ. 2, 348-353.

Appleby, P.G., 2001. Chronostratigraphic techniques in recent sediments. In Last, W.M. and Smol, J.P., editors, *Tracking environmental change using lake sediments volume 1: basin analysis, coring, and chronological techniques*. Kluwer Academic, 171–203.

Babonneau, N., Savoye, B., Cremer, M., Klein, B., 2002. Morphology and architecture of the present canyon and channel system of the Zaire deep-sea fan. Mar. Petrol. Geol. 19, 445-467.

Baudin, F., Disnar, J.R., Martinez, P., Dennielou, B., 2010. Distribution of the organic matter in the channel-levees systems of the Congo mud-rich deep sea fan (West Africa). Implication for deep offshore petroleum source rocks and global carbon cycle. Mar. Petrol. Geol. 27, 995-1010.

Berner, R.A., 1980. Early Diagenesis: A Theoretical Approach. Princeton University Press, Princeton.

Boetius, A., Ravenschlag, K., Schubert, C.J., Rickert, D., Widdel, F., Gieseke, A., Amann, R., Jørgensen, B.B., Witte, U., Pfannkuche, O., 2000. A marine microbial consortium apparently mediating anaerobic oxidation of methane. Nature 407, 623-626.

Bonnel, C., 2005. Mise en place des lobes distaux dans les systèmes turbiditiques actuels : Analyse comparée des systèmes du Zaïre, Var et Rhône. Thèse de Doctorat, Université de Bordeaux I, 275 pp.

Boudreau, B.P. (1998) Mean mixed depth of sediments: the wherefore and the why. Limnol. Oceanogr. 43, 524-526.

Canals, M., Puig, P., Durrieu de Madron, X., Heussner, S., Palanques, A., Fabres, J., 2006. Flushing submarine canyons. Nature 444, doi:10.1038/nature05271.

Caprais, J.C., Lanteri, N., Crassous, P., Noel, P., Bignon, L., Rousseaux, P., Pignet, P., Khripounoff, A., 2010. A new CALMAR benthic chamber operating by submersible: First application in the cold-seep environment of Napoli mud volcano (Mediterranean Sea). Limnol. Oceanogr. Methods 8, 304-312.

Cazala, C., Reyss, J.L., Decossas, J.L., Royer, A., 2003. Improvement in the determination of ^{238}U, $^{228\text{-}234}$Th, $^{226\text{-}228}$Ra, ^{210}Pb, and ^{7}Be by γ spectrometry on evaporated fresh water samples. Environ.l Sci. Technol. 37, 4990-4993.

Cochonat P., 1998. ZAIANGO2 cruise, L'Atalante R/V, http://dx.doi.org/10.17600/98010110

Cochran, J.K. (1985) Particle mixing rates in sediments of the eastern equatorial pacific: Evidence from ^{210}Pb, ^{239,240}Pu and ^{137}Cs distributions at MANOP sites. Geochim. Cosmochim. Acta 49, 1195-1210.

Coynel, A., Seyler, P., Etcheber, H., Meybeck, M. and Orange, D., 2005. Spatial and seasonal dynamics of total suspended sediment and organic carbon species in the Congo River. Glob. Biogeochem. Cycles 19, GB4019, doi:4010.1029/2004GB002335.

Dagg, M., Benner, R., Lohrenz, S., Lawrence, D., 2004. Transformation of dissolved and particulate materials on continental shelves influenced by large rivers: plume processes. Contin. Shelf Res. 24, 833-858.

Dennielou, B., 2002. Rapport Final ZaïAngo: âges et taux d'accumulation du deep-sea fan du Zaïre, synthèse des éléments de stratigraphie, Unpublished report: IFREMER, Brest.

Dennielou et al., this issue.

Degens, E.T., Kempe, S., Richey, J.E., 1991. Summary: biogeochemistry of major world rivers in: Degens, E.T., Kempe, S., Richey, J.E. (Eds.), Biogeochemistry of major world rivers. Wiley and sons, Chichester, pp. 323-348.

Distel, D. L., A. R. Baco, E. Chuang, W. Morrill, C. Cananaugh and C. R. Smith, 2000. Do mussel take wooden steps to deep-sea vents? Nature 403: 725.

Droz, L., Marsset, T., Ondreas, H., Lopez, M., Savoye, B., Spy-Anderson, L., 2003. Architecture of an active mud-rich turbidite system: the Zaire Fan (Congo-Angola margin southeast Atlantic). Results from Zaiango 1 and 2 cruises. ., 87(7): . AAPG Bulletin 87, 1145-1168.

Fiala-Médioni, A., Felbeck, H., 1990. Autotrophic processes in invertebrate nutrition : bacterial symbiosis in bivalve molluscs. Comp. Physiol. 5, 49-69.

Galéron, J., Menot, L., Renaud, N., Crassous, P., Khripounoff, A., Treignier, C., Sibuet, M., 2009. Spatial and temporal patterns of benthic macrofaunal communities on the deep continental margin in the Gulf of Guinea. Deep Sea Res. Part II: Top.l Stud. Oceanogr. 56, 2299.

Goni, M.A., Ruttenberg, K.C., Eglinton, T.I., 1997. Sources and contribution of terrigenous organic carbon to surface sediments in the Gulf of Mexico. Nature 389, 275-278.

Hedges, J.I., Keil, R.G., Benner, R., 1997. What happens to terrestrial organic matter in the ocean? Org. Geochem. 27, 195-212.

Heezen, B.C., Menzies, R.J., Schneider, E.D., Ewing, W.M., Granelli, N.C.L., 1964. Congo Submarine Canyon. AAPG Bulletin 48, 1126–1149.

Heussner, S.,Durrieu de Madron, X., Calafat, A., Canals, M., Carbonne, J., Delsaut, N., Saragoni, G., 2006. Spatial and temporal variability of downward particle fluxes on a continental slope: lessons from an 8-yr experiment in the Gulf of Lions (NW Mediterranean). Mar. Geol. 234, 63-92.

Jahnke, 2010. Global synthesis. In Liu, K.-K., Atkinson, L., Quiñones, R., Talaue-McManus, L. (Eds), Carbon and Nutrient Fluxes in Continental Margins: A Global Synthesis. Springer, Berlin, pp 597-615.

Khripounoff, A., Caprais, J.-C., Crassous, P., 2006. Geochemical and biological recovery of the disturbed seafloor in polymetallic nodule fields of the Clipperton-Clarion Fracture Zone (CCFZ) at 5000m depth. Limnol. Oceanogr. 51, 2033-2041.

Khripounoff, A., Vangriesheim, A., Babonneau, N., Crassous, P., Savoye, B., Dennielou, B., 2003. Direct observation of intense turbidity current activity in the Zaire submarine valley at 4000 m water depth. Mar. Geol. 194, 151-158.

Khripounoff, A., Caprais, J., Crassous, P. and Etoubeau, J., 2006. Geochemical and biological recovery of the disturbed seafloor in polymetallic nodule fields of the Clipperton-Clarion Fracture Zone (CCFZ) at 5,000-m depth. Limnol. Oceanogr. 51, 2033-2041.

Khripounoff, A., Caprais, J.C., Decker, C., Essirard, M., Le Bruchec, J., Noel, P., Olu, K., 2015. Variability in gas and solute fluxes through deep-sea chemosynthetic ecosystems inhabited by vesicomyid bivalves in the Gulf of Guinea. Deep-Sea Res. I 95, 122-130.

Krylova E., Cosel Rv. 2011. A new genus of large Vesicomyidae (Mollusca, Bivalvia, Vesicomyidae, Pliocardiinae) from the Congo margin, with the first record of the subfamily Piocardiinae in the Bay of Biscay (northern Atlantic). *Zoostystema* 33, 83-99.

Krylova EM, Sahling H. 2010. Vesicomyidae (Bivalvia): Current Taxonomy and Distribution. *PLoS ONE* **5**: e9957.

Laraque, A., Bricquet, J.P., Pandi, A. and Olivry, J.C., 2009. A review of material transport by the Congo River and its tributaries. Hydrol. Proc. 23, 3216–3224.

Levin, L.A., Sibuet, M., 2012. Understanding continental margin biodiversity: a new imperative. Ann. Rev. Mar. Sc. 4, 79-112.

Levin, L.A. and Le Bris, N., 2015. The deep ocean under climate change. Science 350, 766-768.

Liu, K.-K., Atkinson, L., Quiñones, R., Talaue-McManus, L., 2010. Carbon and nutrient fluxes in continental margins: a global synthesis. Springer, Berlin, 741p.

Mayer, L.A., Shor, A.N., Clarke, J.H., Piper, D.J.W., 1988. Dense biological communities at 3850 m on the Laurentian Fan and their relationship to the deposits of the 1929 Grand Banks earthquake. Deep Sea Res. (I) 35, 1235-1246.

McKee, B., Aller, R.C., Allison, M.A., Bianchi, T.S., Kineke, G.C., 2004. Transport and transformation of dissolved and particulate materials on continental margins influenced by major rivers: benthic boundary layer and seabed processes. Cont. Shelf Res. 24, 899-926.

Menot, L., Sibuet, M., Carney, R.S., Levin, L.A., Rowe, G.T., Billet, D.S.M., Poore, G., Kitazato, H., Vanreusel, A., Galéron, J., Lavrado, H.P., Sellanes, J., Ingole, B., Krylova, E., 2010. New Perceptions of Continental Margin Biodiversity in: McIntyre, D.A. (Ed.), Life in the World's Oceans. Blackwell Publishing Ltd. pp. 79-101.

Migeon, S., Savoye, B., Babonneau, N., Spy-Anderson, F.-L., 2004. Processes of sediment-waves construction along the present Zaire Deep-sea meandering channel: role of meanders and flow stripping. J. Sed. Res. 74(4), 580-598.

Milliman, J.D., 1991. Flux and fate of fluvial sediment and water in coastal seas, in: Mantoura, R.F.C., J-M. Martin and R. Wollast (Eds.), Ocean margin processes in global change. J. Wiley and sons, Berlin, pp. 69-91.

Mollenhauer, G., Schneider, R.R., Jennerjahn, T., Muller, P.J. and Wefer, G., 2004. Organic carbon accumulation in the South Atlantic Ocean: its modern, mid-Holocene and last glacial distribution. Glob. Planet. Change 40, 249-266.

Monaco, A., Biscaye, P., Soyer, J., Pocklington, R., Heussner, S., 1990. Particle fluxes and ecosystem response on a continental margin: the 1985–1988 Mediterranean ECOMARGE experiment. Cont. Shelf Res. 10, 809-839.

Nelson, D.C., Wirsen, C., Jannasch, W.H., 1989. Characterization of large autotrophic Beggiatoa spp. abundant at hydrothermal vents of the Guaymas Basin. App. Envir.l Microb. 55, 2909-2917.

Niemann, H., Losekann, T., de Beer, D., Elvert, M., Nadalig, T., Knittel, K., Amann, R., Sauter, E.J., Schluter, M., Klages, M., Foucher, J.P., Boetius, A., 2006. Novel microbial communities of the Haakon Mosby mud volcano and their role as a methane sink. Nature 443, 854-858, doi:10.1038/nature05227.

Olu-Le Roy, K., Caprais, J.-C., Fifis, A., Fabri, M.C., Galéron, J., Budzinsky, H., Le Ménach, K., Khripounoff, A., Ondreas, H., Sibuet, M., 2007. Cold-seep assemblages on a giant pockmark off West Africa: spatial patterns and environmental control. Mar. Ecol. Prog. Ser. 28, 115-130.

Olu K., 2011. WACS cruise, Pourquoi Pas? R/V, http://dx.doi.org/10.17600/11030010

Ondréas, H., Olu, K., Fouquet, Y., Charlou, J., Gay, A., Dennielou, B., Donval, J., Fifis, A., Nadalig, T., Cochonat, P., Cauquil, E., Bourillet, J., Moigne, M., Sibuet, M., 2005. ROV study of a giant pockmark on the Gabon continental margin. Geo-Mar. Let. 25 281.

Picot, M., Droz, L., Marsset, T., Dennielou, B., Bez, M., in revision, Controls on turbidite sedimentation: insights from a quantitative approach of channels and lobes architectural parameters (Late Quaternary Congo fan), Mar. Petrol. Geol.

Picot, M., 2015. Cycles sédimentaires dans le système turbiditique du Congo (ex Zaïre) : nature et origine, PhD thesis, Université de Bretagne Occidentale.

Pop Ristova, P., Wenzhöfer, F., Ramette, A., Zabel, M., Fischer, D., Kasten, S., Boetius, A.. 2012. Bacterial diversity and biogeochemistry of different chemosynthetic habitats of the REGAB cold seep (West African margin, 3160 m water depth). Biogeosciences 9, 5031-5048.

Rabouille, C., Mackenzie, F., Ver, L.M., 2001. Influence of the human perturbation on carbon, nitrogen and oxygen biogeochemical cycles in the global coastal ocean. Geochim. Cosmochim. Acta 65, 3615-3639.

Rabouille, C., Caprais, J.C., Lansard, B., Crassous, P., Dedieu, K., Reyss, J.L., Khripounoff, A., 2009. Organic matter budget in the Southeast Atlantic continental margin close to the Congo Canyon: In situ measurements of sediment oxygen consumption. Deep-Sea Res. Part II-Top. Stud. Oceanogr. 56, 2223-2238.

Rabouille C., 2011. CONGOLOBE cruise, Pourquoi Pas? R/V, http://dx.doi.org/10.17600/11030170

Ragueneau, O., Regaudie-de-Gioux, A., Moriceau, B., Gallinari, M., Vangriesheim, A., Baurand, F., Khripounoff, A., 2009. A benthic Si mass balance on the Congo margin: Origin of the 4000 m DSi anomaly and implications for the transfer of Si from land to ocean. Deep Sea Research Part II: Topical Studies in Oceanography 56, 2197.

Raimonet, M., Ragueneau, O., Jacques, V., Corvaisier, R., Moriceau, B., Khripounoff, A., Pozzato, L., Rabouille, C., 2015. Rapid transport and high accumulation of amorphous silica in the Congo deep-sea fan: a preliminary budget. J. Mar Sys. 141, 71-79.

Reyss, J.L., Schmidt, S., Legeuleux, F., Bonte, P., 1995. Large low background well-type detectors for measurements of environmental radioactivity. Nucl. Instr. Methods 357, 391-397.

Sanchez-Vidal, A., Canals, M., Calafat, A., Lastras, G., Pedrosa-Pamiers, R., Menendez, M., Medina, R., Company, J.B., Hereu, B., Romero, J. and Alcoverro, T. (2012) Impacts on the Deep-Sea Ecosystem by a Severe Coastal Storm. PLoSONE 7(1): e30395, doi:10.1371/journal.pone.0030395.

Savoye, B., Babonneau, N., Dennielou, B., Bez, M., 2009. Geological overview of the Angola-Congo margin, the Congo deep-sea fan and its submarine valleys. Deep-Sea Res. Part II-Top. Stud. Oceanogr. 56, 2169.

Savoye, B., Cochonat, P., Apprioual, R., Bain, O., Baltzer, A., Bellec, V., Beuzart, P., Bourillet, J., Cagna, R., Cremer, M., Crusson, A., Dennielou, B., Diebler, D., Droz, L., Ennes, J., Floch, G., Foucher, J., Guiomar, M., Harmegnies, F., Kerbrat, R., Klein, B., Khun, H., Landure, J., Lasnier, C., Le Drezen, E., Le Formal, J., Lopez, M., Loubrieu, B., Marsset, T., Migeon, S., Normand, A., Nouze, H., Ondreas, H., Pelleau, P., Saget, P., Seranne, M., Sibuet, J.C., Tofani, R., Voisset, M., 2000. Structure et évolution récente de l'éventail turbiditique du Zaïre: Premiers résultats scientifiques des missions d'exploration ZaiAngo 1 and 2 (Marge Congo-Angola). C. R. Acad. Sci. Paris 311, 211-220.

Savoye B., Ondreas H., 2000. ZAIANGOROV cruise, L'Atalante R/V, http://dx.doi.org/10.17600/10100

Savoye B., 1998. ZAIANGO1 cruise, L'Atalante R/V, http://dx.doi.org/10.17600/98010100

Schlunz, B., Schneider, E.D., Muller, P.J., Showers, W.J., Wefer, G., 1999. Terrestrial organic carbon accumulation on the Amazon deep-sea fan during the last glacial sea level low stand. Chem. Geol. 159, 263–281.

Schlunz, B., Schneider, R.R., 2000. Transport and terrestrial organic carbon to the oceans by rivers: re-estimating flux and burial rates. Int. J. Earth Sci. 88, 599-606.

Sibuet, M., Olu, K., 1998. Biogeography, biodiversity and fluid dependence of deep-sea cold-seep communities at active and passive margins. Deep-Sea Res. Part II-Top. Stud. Oceanogr. 45, 517-567.

Sibuet, M., Vangriesheim, A., 2009. Deep-sea environment and biodiversity of the West African Equatorial margin. Deep-Sea Res. Part II-Top. Stud. Oceanogr. 56, 2156.

Simeoni, P., Sarrazin, J., Nouze, H., Sarradin, P.M., Ondreas, H., Scalabrin, C., Sinquin, J.M. 2007. Victor 6000: New high resolution tools for deep-sea research. Oceans 2007 - Europe, Vols 1-3. IEEE, New York, 133-138 pp.

Smith, C.R., Kukert, H., Wheatcroft, R.A., Jumars, P.A., Deming, J.W.. 1989. Vent fauna on whale remains. Nature 341, 27-28.

Spencer, R.G.M., Hernes, P.J., Aufdenkampe, A.K., Baker, A., Gulliver, P., Stubbins, A., Aiken, G.R., Dyda, R.Y., Butler, K.D., Mwambai, V.L., Mangangu, A.M., Wabakanghanzi, J.N. and Six, J., 2012. An initial investigation into the organic matter biogeochemistry of the Congo River. Geochim. Cosmochim. Acta 84, 614–627.

Spitzy, A., Ittekkot, V., 1991. Dissolved and particulate organic matter in rivers, in: Mantoura, R.F.C., J-M. Martin and R. Wollast (Eds.), Ocean margin processes in global change. J. Wiley and sons, Berlin, pp. 5-17.

Stetten, E., Baudin, F., Reyss, J.L., Martinez, P., Charlier, K., Schnyder, J., Rabouille, C., Dennielou, B., Coston-Guarini, J., Pruski, A., 2015. Organic matter characterization and distribution in sediments of the terminal lobes of the Congo deep-sea fan: evidence for the direct influence of the Congo River. Mar. Geol. 369, 182-195.

Teixeira, S., Olu, K., Decker, C., Cunha, R.L., Fuchs, S., Hourdez, S., Serrão, E.A., Arnaud-Haond, S., 2013. High connectivity across the fragmented chemosynthetic ecosystems of the deep Atlantic Equatorial Belt: efficient dispersal mechanisms or questionable endemism? Molec. Ecol. 22, 4663-4680.

Tesi, T., Goni, M.A., Langone, L., Puig, P., Canals, M., Nittrouer, C., Durrieu de Madron, X., Calafat, A., Palanques, A., Heussner, S., Davies, M.H., Drexler, T.M., Fabres, J. and Miserocchi, S., 2010. Reexposure and advection of 14C ‐ depleted organic carbon from old deposits at the upper continental slope. Glob. Biogeochem. Cycles 24, GB4002, doi:4010.1029/2009GB003745.

Treignier, C., Derenne, S., Saliot, A., 2006. Terrestrial and marine n-alcohol inputs and degradation processes relating to a sudden turbidity current in the Zaire canyon. Org. Geochem. 37, 1170-1184.

Turnewitsch, R., Reyss, J.-L., Nycander, J., Waniek, J.J., Lampitt, R.S., 2008. Internal tides and sediment dynamics in the deep sea - Evidence from radioactive $^{234}Th/^{238}U$ disequilibria. Deep-Sea Res I 55, 1727-1747. doi: 10.1016/j.dsr.2008.07.008

Ulses, C., Estournel, C., Durrieu de Madron, X., Palanques, A., 2008. Suspended sediment transport in the Gulf of Lions (NW Mediterranean): Impact of extreme storms and floods. Cont. Shelf Res. 28, 2048-2070, doi:2010.1016/j.csr.2008.2001.2015.

Van Gaever, S., Galéron, J., Sibuet, M., Vanreusel, A., 2009. Deep-sea habitat heterogeneity influence on meiofaunal communities in the Gulf of Guinea. Deep-Sea Res. Part II-Top. Stud. Oceanogr. 56, 2259-2269.

Vangriesheim, A., Khripounoff, A., Crassous, P., 2009a. Turbidity events observed in situ along the Congo submarine channel. Deep-Sea Res. Part II-Top. Stud. Oceanogr. 56, 2208-2222.

Vangriesheim, A., Pierre, C., Aminot, A., Metzl, N., Baurand, F. and Caprais, J.C. 2009b. The influence of Congo River discharges in the surface and deep layers of the Gulf of Guinea. Deep-Sea Res. Part II-Top. Stud. Oceanogr. 56, 2183-2196.

Ver, L.M., Mackenzie, F.T., Lerman, A., 1999. Biogeochemical responses of the carbon cycle to natural and human perturbations: past, present, and future. Amer. J. Sci. 299, 762-801.

Vigneron, A., Cruaud, P., Pignet, P., Caprais, JC., Cambon-Bonavita, MA., Godfroy, A., Toffin, L ., 2013. Archaeal and anaerobic methane oxidizer communities in the Sonora Margin cold seeps, Guaymas Basin (Gulf of California). ISME Journal 7, 1595-1608.

Walsh, J.J., 1988. On the nature of continental shelves. Academic press, London.

Wollast, R., 1993. Interactions of carbon and nitrogen cycles in the coastal zone, in: Wollast, R., Mackenzie, F.T., Chou, L. (Eds.), Interactions of C, N, P and S biogeochemical cycles and global change. Springer-Verlag, Berlin, pp. 195-210.

Wollast, R., 1998. Evaluation and comparison of the global carbon cycle in the coastal zone and in the open ocean, in: Brink, K.H., Robinson, A.R. (Eds.), The Sea. Wiley & sons, New York, pp. 213-252.

Annexe: Position of operations

Calypso cores

Date	Time	Lat (°S)	Long (°E)	Label	Station	Depth (m)
24/02/2011	19:35	6°44'18.4	5°19'35.8	WACS-CS06	D	4996
25/02/2011	21:05	6°42'08.5	5°29'18.4	WACS-CS07	C	4955
18/12/2011	23:42	6°27'45.3	6°01'55.0	CoL-A-CS01	A	4755
20/12/2011	11:04	6°28'18.6	6°02'09.0	CoL-A-CS02	A	4763
23/12/2011	16:37	6°34'55.6	5°41'37.2	CoL-F-CS03	F	4866
29/12/2011	15:20	6°39'37.2	5°28'10.1	CoL-C-CS04	C	4949
30/12/2011	22:29	6°41'57.0	5°29'19.7	CoL-C-CS05	C	4955
02/01/2012	13:28	6°41'57.0	5°29'19.8	CoL-C-CS06	C	4954
05/01/2012	17:49	6°25'36.7	5°49'34.5	CoL-C-CS07	B	4822

Multicores

Date	Time	Lat (°S)	Long (°E)	Label	Station	Depth (m)
20/02/2011	11:16	6°27'15.6	6°01'56.0	WACS-A-MTB3	A	4884
22/02/2011	7:20	6°41'15.7	5°29'00.0	WACS-C-MTB4	C	4955
23/02/2011	11:29	6°41'15.1	5°28'59.4	WACS-C-MTB5	C	4953
25/02/2011	16:50	6°41'15.9	5°28'59.8	WACS-C-MTB6	C	4956
18/12/2011	19:09	6°27'35.9	6°02'04.7	CoL-A-MTB2	A	4759
20/12/2011	4:32	6°28'12.5	6°02'12.9	CoL-A-MTB3	A	4774
21/12/2011	11:44	6°34'51.0	5°41'27.4	CoL-F-MTB4	F	4864
23/12/2011	12:31	6°34'50.0	5°41'27.9	CoL-F-MTB5	F	4864
25/12/2011	19:03	6°40'15.9	5°28'24.0	CoL-C-MTB6	C	4951
28/12/2011	9:13	6°34'49.9	5°41'27.8	CoL-F-MTB7	F	4861
29/12/2011	11:17	6°40'16.1	5°28'23.8	CoL-C-MTB8	C	4950
30/12/2011	13:42	6°40'16.0	5°28'25.6	CoL-C-MTB9	C	4950
31/12/2011	2:34	6°41'57.0	5°29'19.7	CoL-C-MTB10	C	4954
31/12/2011	6:28	6°41'56.8	5°29'19.8	CoL-C-MTB11	C	4960
04/01/2012	13:42	6°25'36.9	5°49'35.2	CoL-B-MTB12	B	4823
05/01/2012	22:54	6°27'35.6	6°02'04.5	CoL-A-MTB13	A	4767
06/01/2012	7:52	6°05'53.6	5°54'29.0	CoL-E-MTB14	E	4750

Respirometer deployments

Date	Time	Lat (°S)	Long (°E)	Label	Station	Depth (m)
20/02/2011	4:02	6°27'14.7	6°01'58.4	WACS-A-RAP3	A	4765
22/02/2011	9:14	6°41'15.9	5°29'01.6	WACS-C-RAP4	C	4953
16/12/2011	17:00	6°27'36.1	6°02'04.6	CoL-A-RAP1	A	4759
23/12/2011	8:38	6°34'54.3	5°41'27.8	CoL-F-RAP2	F	4873
26/12/2011	14:29	6°40'09.0	5°28'23.1	CoL-C-RAP3	C	4945
31/12/2011	7:41	6°41'56.8	5°29'19.8	CoL-C-RAP4	C	4955
04/01/2012	13:25	6°25'42.0	5°49'51.7	CoL-B-RAP5	B	4827

DMPS deployments

Date	Time	Lat (°S)	Long (°E)	Label	Station	Depth (m)
24/02/2011	2:08	6°42'04.7	5°29'17.3	WACS-C-DPMS4	C	4946
30/12/2011	05:40	6°41'23.3	5°28'46.7	CoL-C-DMPS3	C	4946
03/01/2012	03:09	6°42'11.9	5°29'17.7	CoL-C-DMPS4	C	4946

Markers

Date	Time	Lat (°S)	Long (°E)	Label	Station	Dive	Depth (m)
20/02/2011	18:55:05	6°26'54.4	6°01'55.8	W11	A	PL435	4751
22/02/2011	16:41:53	6°42'45.9	5°29'25.8	W12	C	PL436	4946
24/02/2011	02:47:15	6°42'04.7	5°29'17.2	W15	C	PL437	4945
25/02/2011	08:56:58	6°47'32.9	5°12'47.3	W13	D	PL438	5028
19/12/2011	11:55	6°28'17.0	6°02'08.6	CoL1	A	PL483	4767
20/12/2011	23:21	6°28'16.8	6°02'08.4	CoL2	A	PL484	4769
24/12/2011	9:03	6°35'25.8	5°41'24.7	CoL3	F	PL486	4868
30/12/2011	1:19	6°40'56.9	5°28'55.2	CoL8	C	PL489	4947
30/12/2011	1:41	6°40'54.5	5°28'51.7	CoL6	C	PL489	4944
01/01/2012	10:13	6°41'23.4	5°28'47.0	CoL4	C	PL490	4947
03/01/2012	01:27	6°42'04.9	5°29'17.4	CoL9	C	PL491	4945
03/01/2012	17:30	6°42'13.1	5°29'19.0	CoL10	C	PL491	4946
05/01/2012	3:10	6°25'14.1	5°49'42.8	CoL11	B	PL492	4816
05/01/2012	5:30	6°25'13.1	5°49'42.9	CoL12	B	PL492	4816

Sediment trap

Date	Time	Lat (°S)	Long (°E)	Label	Station	Depth (m)
26/02/2011	6 :42	6°28'03.6	6°02'10.1	WACS-A-PPART03	A	4779

Tables

Table 1: Operations conducted during WACS and Congolobe cruises

	Operation	Reference instrument	Achieved
Ship-operated tools	Multicoring	Oktopus – 8 tubes	17
	Piston coring	Calypso – 5-25 meters (Institut Paul Emile Victor, IPEV)	9
	Respirometer	RAP2 - IFREMER	7
	Sediment trap and ADCP current meter	Technicap PPS5 + RDI 300kHz ADCP	1
ROV-operated tools	High- Resolution Bathymetry	Reson Seabat 7125	3 stations
	Bottom imagery	OTUS camera	3 stations
	Sediment and fauna sampling		
	- Pushcores	CT-Ifremer/Victor 6000	12 dives
	- Aspirator	ASPI-Ifremer/Victor 6000	"
	- Blade cores	GCL or CL-Ifremer/Victor 6000	"
	- Water sampler	PEP-Victor 6000	"
	- Nets	Ifremer/Victor 6000	"
	Benthic incubation chambers	CALMAR Ifremer	"
	In situ Profiler	DMPS-Unisense/Ifremer	3

Table 2: Details of bathymetric ROV acquisitions on each site

Sites	A		F		C	
ROV speed (m/s)	0.3-0.4					
ROV altitude (m)	60	8	60	8	60	8
Parallel profiles spacing (m)	180	*n.a.*	180	*n.a.*	180	5
Number of parallel profiles (mosaics)	8	*n.a.*	5	*n.a.*	6	18
Mosaic size (length km x width km)	3.6 x 0.7-1.5	*n.a.*	2.8 x 1.0-1.7	*n.a.*	6.2 x 0.8	
Total number of profiles	9	1	10	1	7	21
Total length (km)	21.6	23.4	25.2	18.8	30.6	30.4

Table 3: Position of the 6 Congolobe and WACS sites and official operation labels (PL stands for ROV dive; MTB for Multicore; CS for Calypso core; RAP for Autonomous benthic chamber; DMPS for in situ microprofiler; PPART for sediment trap deployment). Note that labels on maps are simplified (excluding station name and replacing WACS by W) for clarity of the Figures.

	Long (°S)	Lat (°E)	Depth (m)	Sampling dives	Sampling	RAP-DMPS
Site A	6°28'S	6°02'E	4765	PL435 PL483-484	CoL-A-MTB2-3-13 WACS-A-MTB3 CoL-A-CS01-02	CoL-A-RAP1 WACS-A-RAP3 WACS-A-PPART3
Site B	6°25'S	5°49'E	4840	PL492	CoL-B-MTB12 CoL-B-CS07	CoL-B-RAP5
Site F	6°35'S	5°42'E	4875	PL486	CoL-F-MTB4-5-7 CoL-F-CS03	CoL-F-RAP2
Site C	6°42'S	5°29'E	4950	PL436-437 PL489-490-491	CoL-C-MTB6-8-9-10-11 WACS-C-MTB4-5-6 CoL-C-CS04-05-06 WACS-CS07	CoL-C-RAP3-4 WACS-C-RAP4 WACS-C-DMPS4 CoL-C-DMPS3-4
Site D	6°46'S	5°16'E	5030	PL438	WACS-CS06	/
Site E	6°06'S	5°54'E	4765	PL494	CoL-E-MTB14	/

Table 4: Sedimentation rates at the Congolobe/WACS/ZAIANGO sites

Site	$^{210}Pb_{xs}$ Sedimentation rate (cm yr^{-1})	^{137}Cs Sedimentation rate (cm yr^{-1})
A	0.6	1
C	22	12
KZAI7	/	>2.5
KZAI8 (levee)	/	0.7
B	0.4	0.3
KZAI9	/	0.4
KZAI12	/	<0.05
E	/	<0.05

Figure captions

Figure 1: General map of the lobe complex, distal part of the Congo turbidite system with location of the 6 sites explored during WACS and Congolobe cruises: Boxes are the size of Fig. 2 for Site A, Fig. 3 for site B, Fig. 4 for site F, Fig. 5 for site C, Fig. 6 for site D and Fig. 7 for site E. Some previous cores from Zaiango cruises (KZAI) are also shown. Numbers 1 to 5 correspond to lobe number from oldest to youngest (redrawn and simplified from Babonneau, 2002). Dashed lines are individual lobe limits whereas the dotted line is the limit of the channel terminal part, a deposition zone with highest sedimentation rates.

Figure 2: High-resolution bathymetry of site A, included on the low resolution bathymetric map with location of operations, dive tracks (light gray WACS-PL435, dark grey CoL-PL483 and black -PL484) and markers. Note simplified labels (excluding station name and replacing WACS by W) for clarity of the Figures.

Figure 3: Low-resolution bathymetry of site B (distal part of lobe 3) with surface operations, dive track (PL492) and ROV sampling markers. Note simplified labels (excluding station name and replacing WACS by W) for clarity of the Figures.

Figure 4: High-resolution bathymetry of site F included on the low resolution bathymetric map with surface operations, dive track (PL486) and sampling markers. Note simplified labels (excluding station name and replacing WACS by W) for clarity of the Figures.

Figure 5: High-resolution bathymetry of site C included on the low resolution bathymetric map with surface operations, dive tracks (PL436, PL437, PL 489, PL490, PL491) and sampling markers. Note simplified labels (excluding station name and replacing WACS by W) for clarity of the Figures.

Figure 6: Low-resolution bathymetry of site D with Calypso coring, dive track (PL 438) and sampling marker. Note simplified labels (excluding station name and replacing WACS by W) for clarity of the Figures.

Figure 7: Low-resolution bathymetry of site E with multicore and dive track (PL494). Note simplified labels (excluding station name and replacing WACS by W) for clarity of the Figures.

Figure 8: Ecosystems at site A: (a) patch of vesicomyid bivalves observed and sampled in the southern flank of the active channel during PL 483-484 near marker CoL2, (b) patch of vesicomyid bivalves sampled on the northern levee during PL 435 and (c) Reduced sediment with dead vesicomyid shells near marker CoL1 “King Kong” (PL 483-484). See Table 1 for label significance.

Figure 9: Bacterial mats at site F with vesicomyid bivalves observed and sampled during PL 486 near marker CoL3.

Figure 10: Sparse vesicomyid habitats observed near marker CoL11 and CoL12 at site B during dive PL492

Figure 11 : Ecosystems at site C: (a) Dense bacterial mat near marker W12 (PL436), (b) Sparse bacterial mat near marker CoL4 (PL490), (c) Reduced sediments with empty shells of vesicomyids near marker (PL490) known as the “Black Ogre”, (d) vesicomyid “heart” observed and sampled near marker CoL9 during PL491 and (e) vesicomyid “mouth” observed and sampled near W15 during PL437.

Figure 12: $^{210}Pb_{xs}$ and ^{137}Cs profiles in multitube (MTB) and Calypso (CS) cores sampled during the Congolobe cruise (Site A, B, C and E) and during the Zaiango cruise (KZAI 07-09 and 12) from the Congo Deep-sea fan zone. The black straight line represents the regression obtained by the CFCS model for cores from the Congolobe cruise (see methods for details).

Figures

Fig. 1

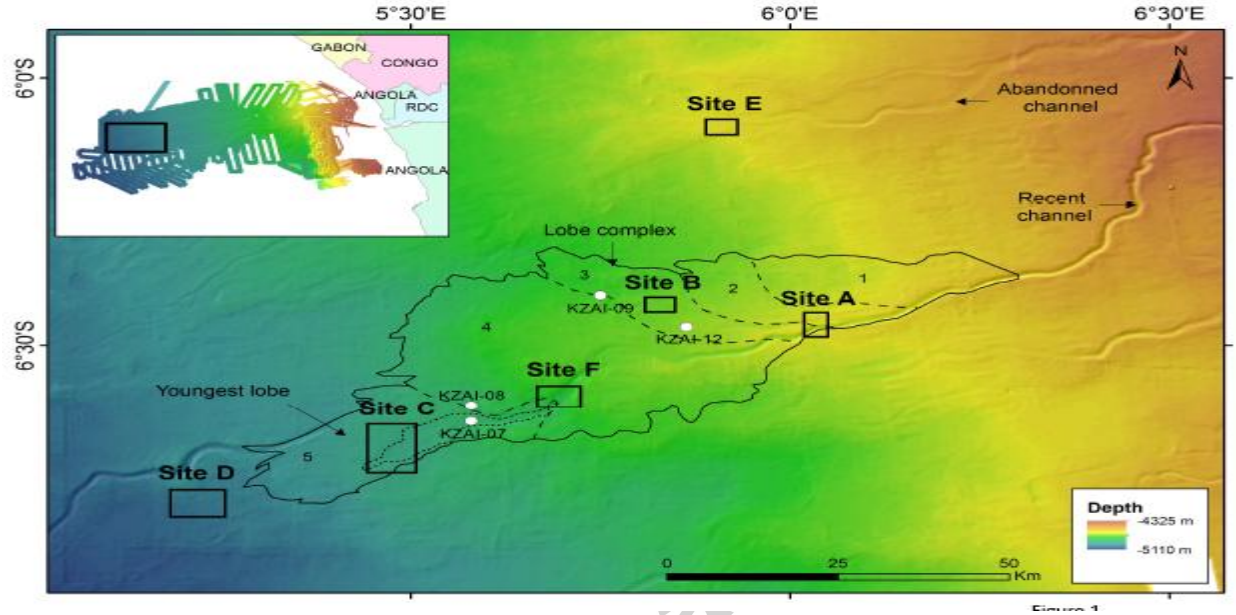

Fig. 2

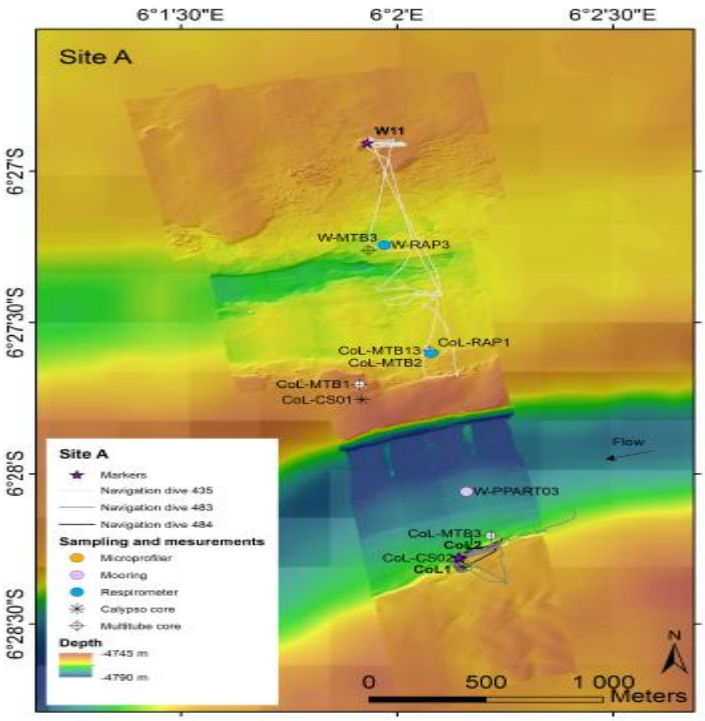

Fig. 3

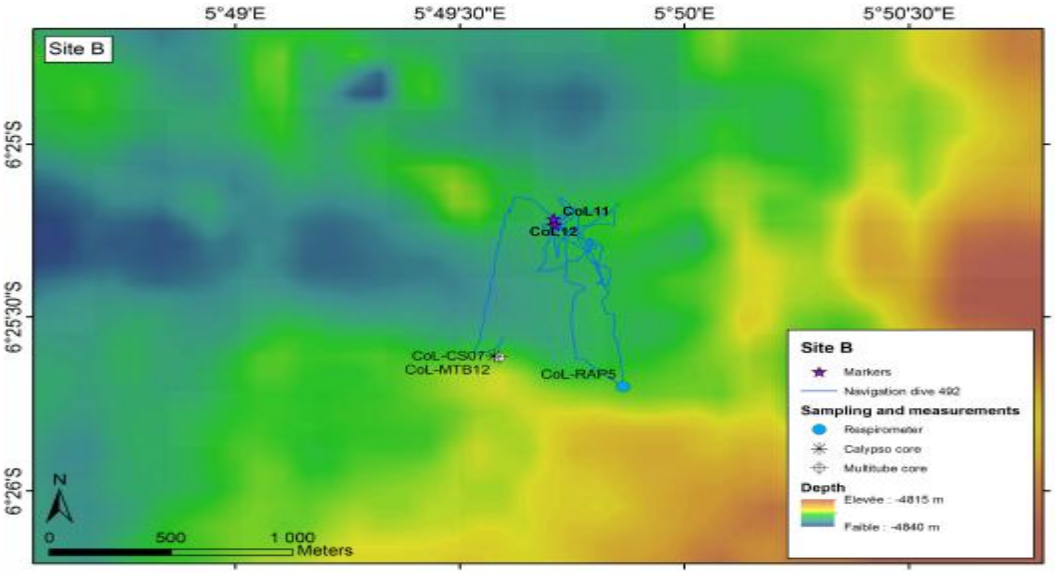

Fig. 4

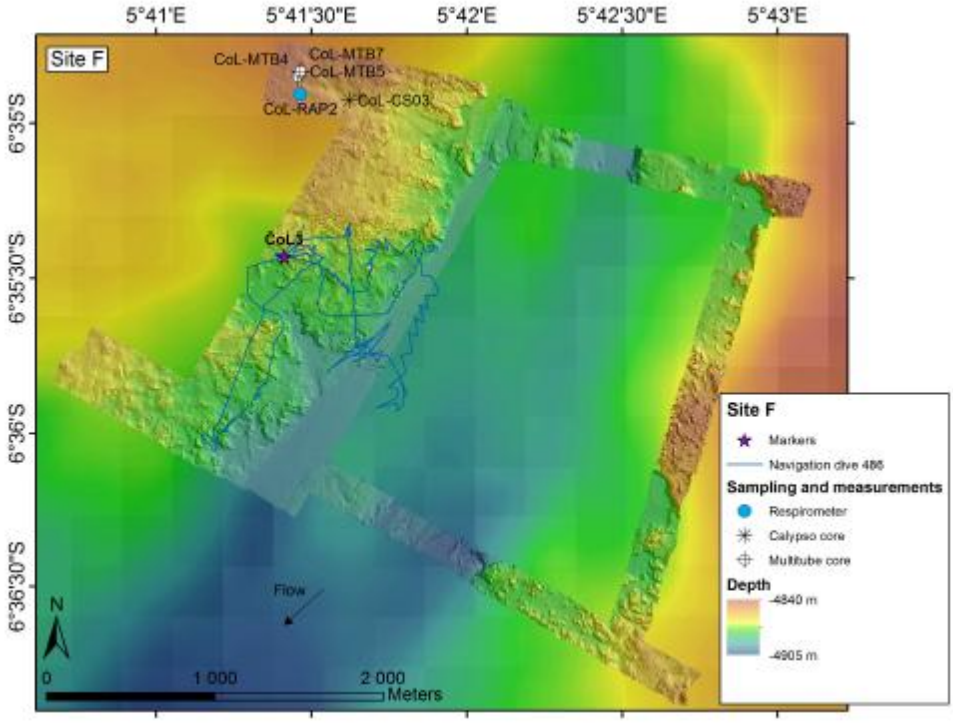

Fig. 5

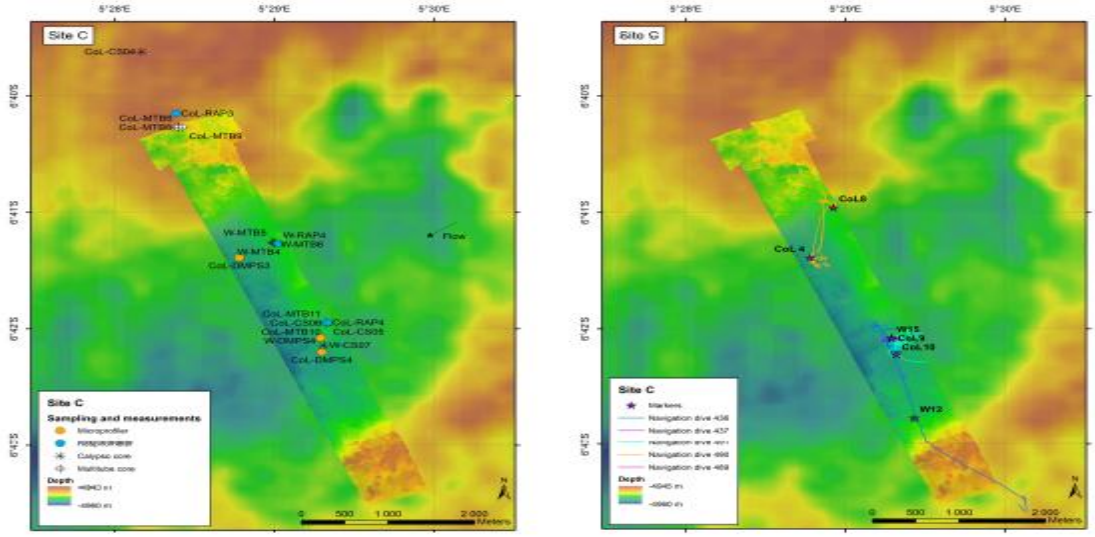

Fig. 6

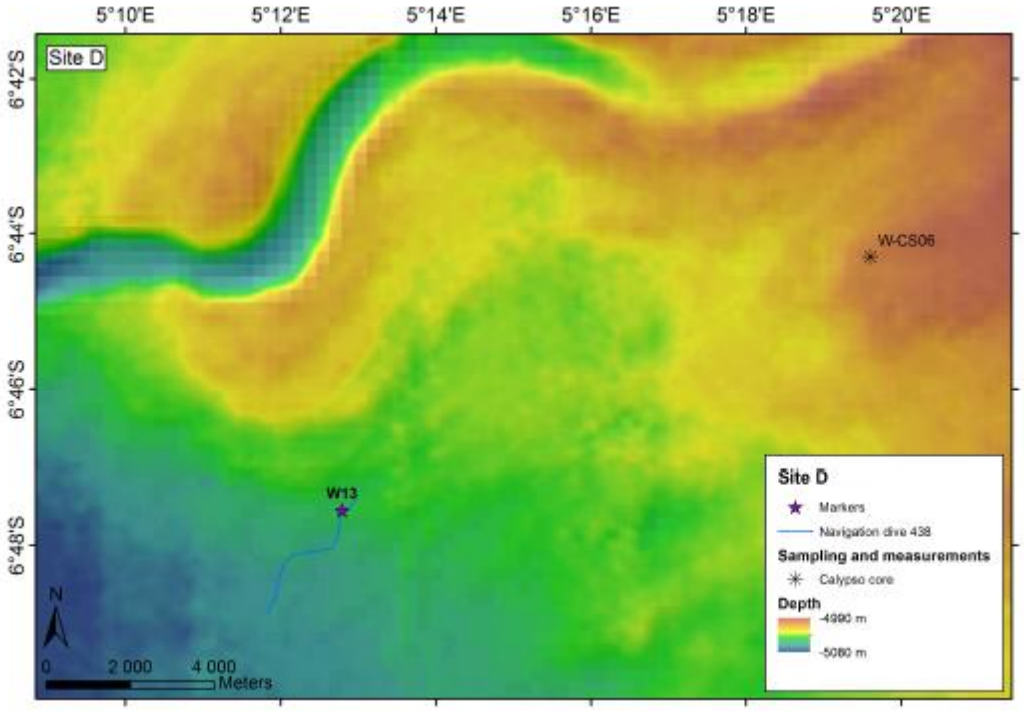

Fig. 7

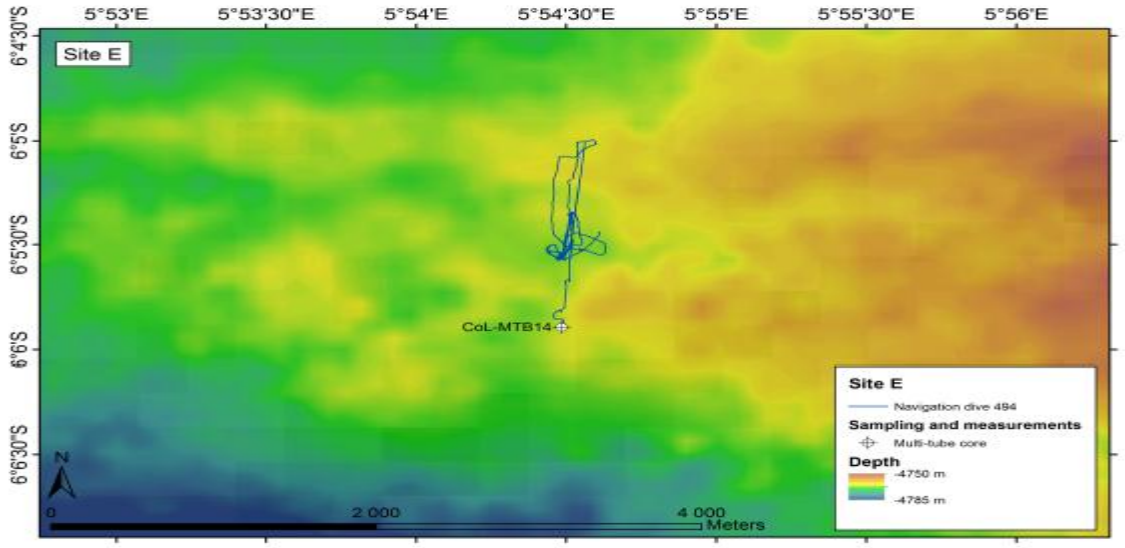
5°53'E
5°53'30"E
5°54'E
5°54'30"E
5°55'E
5°55'30"E
5°56'E
6°4'30"S
6°5'S
6°5'30"S
6°6'S
6°6'30"S
Site E
CoL-MTB14
Site E
Navigation dive 494
Sampling and measurements
Multi-tube core
Depth
-4750 m
-4785 m
N
0
2 000
4 000
Meters

Fig. 8

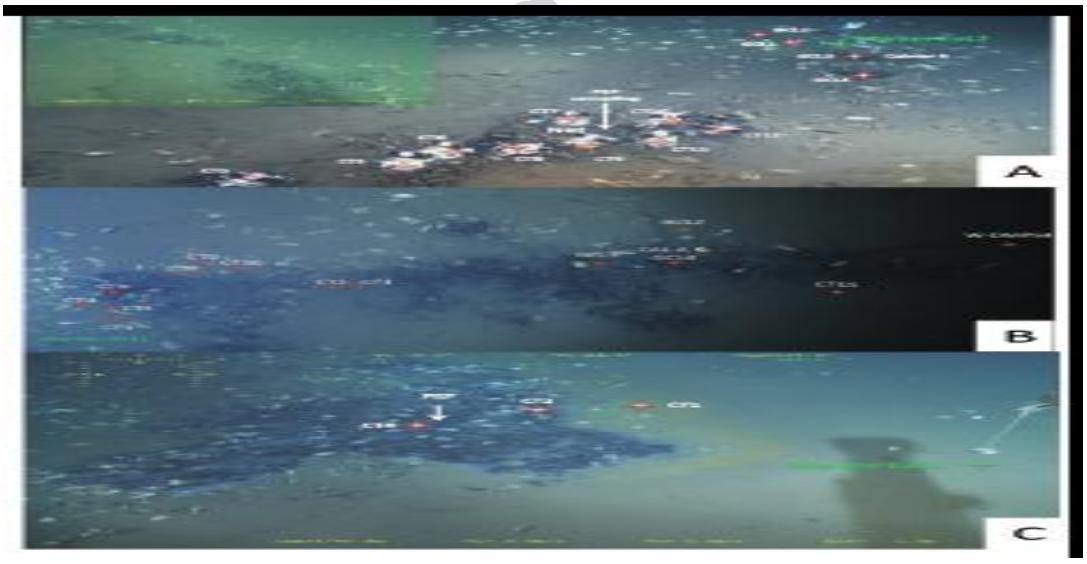
A
B
C

Fig. 9

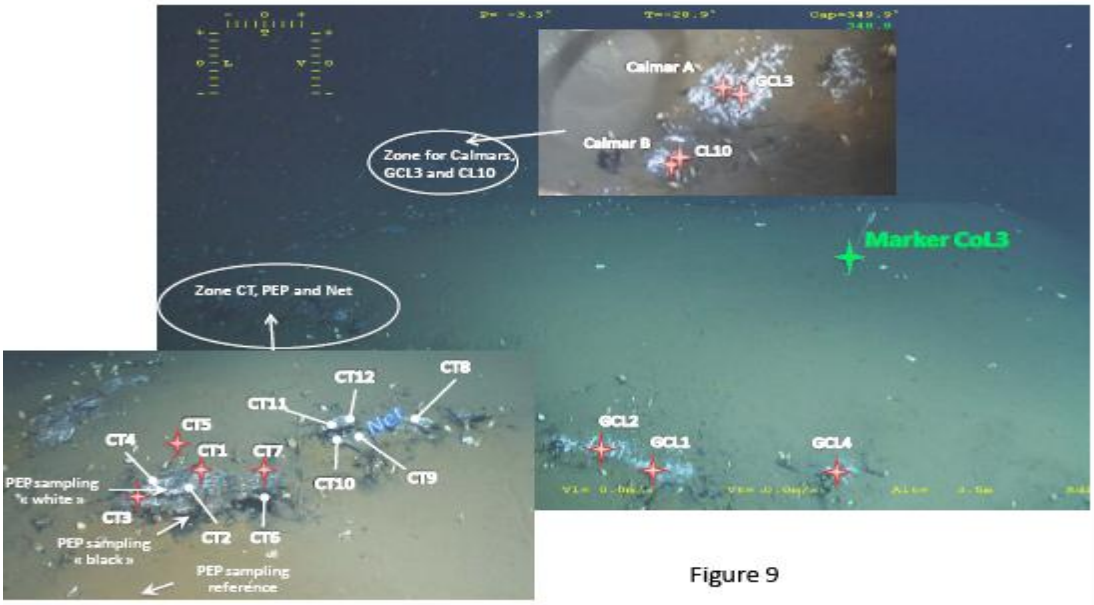

Figure 9

Fig. 10

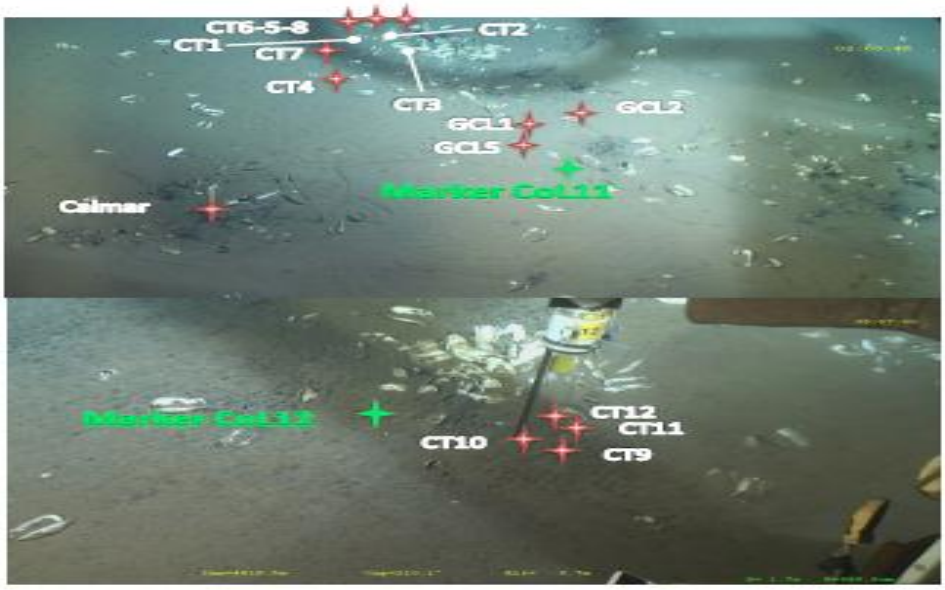

Fig. 11

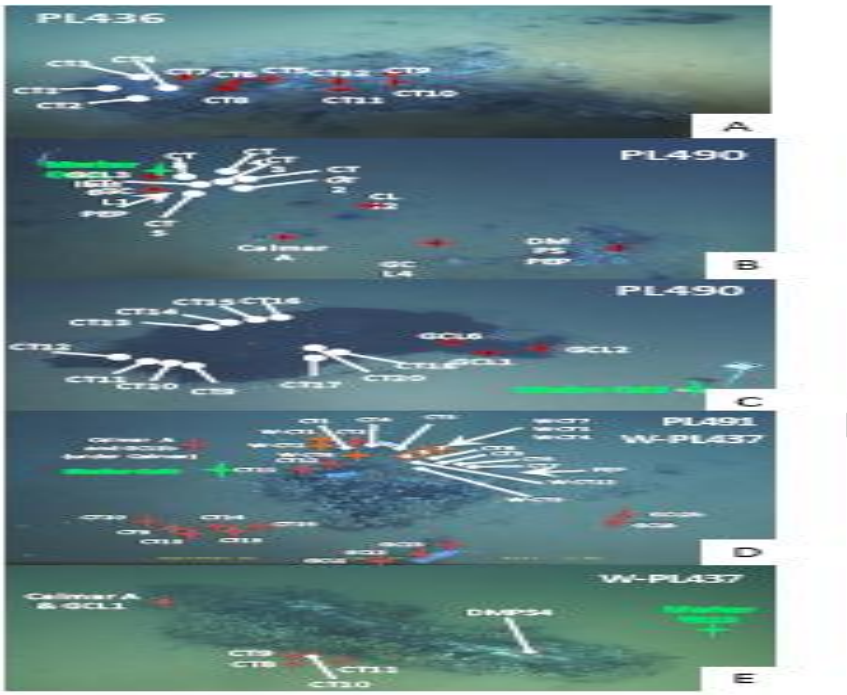

Fig. 12

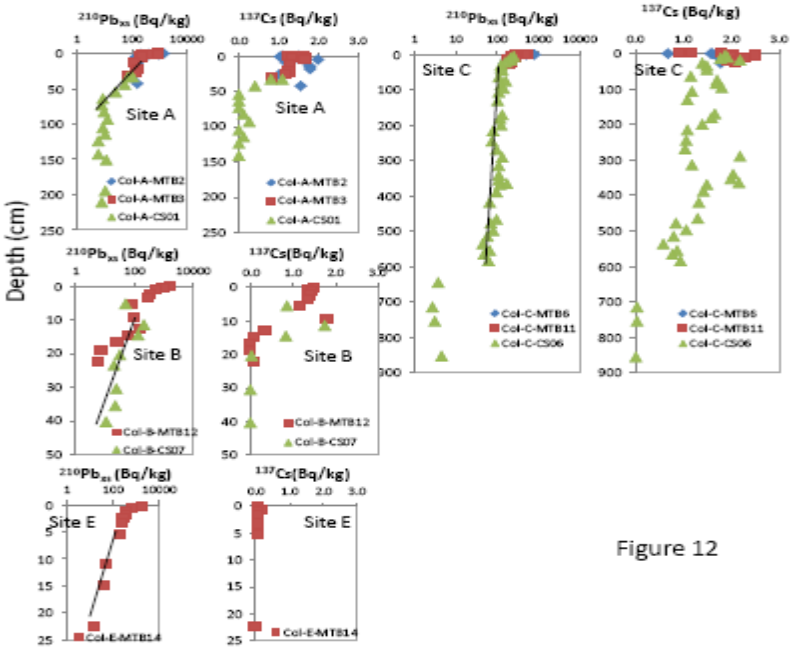

Figure 12